https://doi.org/10.5194/egusphere-2026-5047
Preprint. Discussion started: 26 August 2026

The impact of blowing snow above sea ice on atmospheric ice nucleating particles in the Central Arctic

Megan Malpas[1,2], Floortje van den Heuvel[1], Rachael H. Rhodes[2], Xin Yang[1], Shaun Miller[1], Manuela van Pinxteren[3], Sebastian Zeppenfeld[3], and Markus M. Frey[1]

[1]British Antarctic Survey, Natural Environment Research Council, Cambridge, UK
[2]Department of Earth Sciences, University of Cambridge, Cambridge, UK
[3]Atmospheric Chemistry Department (ACD), Leibniz Institute for Tropospheric Research, Leipzig, Germany

Correspondence: Megan Malpas (megma57@bas.ac.uk) and Markus M. Frey (maey@bas.ac.uk)

Abstract.

Ice nucleating particles (INPs) in the Central Arctic contribute to local climate feedback mechanisms through their impacts on cloud radiative properties and formation. Despite their importance, the contributions of local and remote aerosol sources to Arctic INP populations are currently poorly understood. One potential source of INPs during winter and spring is the sublimation of snow particles during blowing snow events (BSEs) over sea ice, which could constitute a significant local source in an otherwise remote region. We investigated the impact of BSEs on Central Arctic INPs using year-round observations taken during the Multidisciplinary drifting Observatory for the Study of Arctic Climate (MOSAiC) campaign from October 2019 to October 2020. Based on our observations of atmospheric INP and surface snow samples as well as their major ion composition we did not find an impact of BSEs on INP concentrations, but we did observe an increase in INP activation temperatures. Additionally, we found overlapping INP activation temperatures in both surface snow and aerosol, and observed that BSEs brought the enrichment factors of SO_4^{2-}, K^+, and Br^- with respect to Na^+ closer to those observed in surface snow, indicating that sublimating snow is a source of non-sea-salt aerosol. However, our analysis also indicates contributions from long-range transportation during BSEs. We conclude that aerosol populations during BSEs are influenced by a case-dependant combination of sublimating snow and long-range transportation, and we recommend that further work at a higher temporal resolution is needed to fully understand the impact of BSEs on INPs.

1 Introduction

The Arctic is the fastest warming region on Earth, at rates nearly four times greater than the global average (Rantanen et al., 2022). This phenomenon, known as Arctic Amplification, is the result of a complex web of atmosphere-ocean-cryosphere feedback mechanisms (Overland et al., 2019; Serreze and Barry, 2011), most notably in the form of substantial sea ice loss contributing to a decreasing surface albedo. Aerosol also impact the Arctic surface energy budget, through direct radiative effects by absorbing and reflecting radiation, and indirect radiative effects by altering cloud formation and properties (Lubin and Vogelmann, 2006) such as phase, lifetime (Albrecht, 1989), and reflectivity (Twomey, 1977), and represent a major uncertainty in our understanding of Arctic Amplification (Schmale et al., 2021). Low-level mixed phase clouds impact the surface

https://doi.org/10.5194/egusphere-2026-5047
Preprint. Discussion started: 26 August 2026

energy budget through both short-wave and long-wave radiation, and their properties are governed by atmospheric concentrations of a subset of aerosol known as cloud condensation nuclei (CCNs) and ice nucleating particles (INPs), which facilitate water droplet and ice crystal formation respectively (Kanji et al., 2017). In particular, INPs represent only a small fraction of total atmospheric aerosol, with Li et al. (2025), for example, observing 1 in 10^5 aerosol particles acting as INPs at -15 °C, but they disproportionally influence the phase of clouds, as ice crystals grow at the expense of water droplets through the Wegener–Bergeron–Findeisen process (Korolev and Field, 2008). In regions with low baseline aerosol concentrations, such as the Arctic, even small alterations to INP concentrations and species can have a profound impact on cloud phase, and resultant cloud radiative properties (Morrison et al., 2011; Eirund et al., 2019).

Despite this, INP sources and concentrations in the Arctic are poorly understood, with few studies capturing seasonal change, and even fewer occurring in marine regions dominated by sea ice (Schmale et al., 2021). The Arctic aerosol regime has a distinct seasonal cycle, with aerosol mass concentrations peaking during the springtime Arctic haze period, during which an expansion of the polar front allows for long-range transportation of anthropogenic aerosol from lower latitudes (Shaw, 1995). A retreat of that same polar front in summer results in a seasonal minimum in aerosol mass concentration, but a maximum in total number concentration, with a shift to locally-sourced ultrafine aerosol from the open ocean as sea ice coverage decreases and biological productivity increases (Ström et al., 2003). Whether INP concentrations follow the same seasonal cycle as overall aerosol concentrations is not yet known in detail, as only a small number of year-round INP studies in the Central Arctic exist in the literature. Year-round studies at Arctic terrestrial sites can be found in Tobo et al. (2024), Wex et al. (2019), and Freitas et al. (2023), with broad agreement across sites regarding concentrations, and increases in INPs with warmer activation temperatures (> -15 °C) during the summer season. More recently, Creamean et al. (2022) is the first study to present a year-round dataset of INPs above the Arctic Ocean, taken during the Multidisciplinary drifting Observatory for the Study of Arctic Climate (MOSAiC) campaign. They reported INP concentrations at a 3-day resolution and found a strong seasonality, with higher concentrations observed during summer and associated with marine biological productivity, and lower concentrations during winter and spring. This dataset was further analysed in Barry et al. (2025), who found good agreement between the INP concentrations measured during MOSAiC and INPs measured at a terrestrial site at Zeppelin Observatory in Svalbard, suggesting that the INP populations at these sites were influenced by a variety of mixed sources with broad regional influence.

Globally, sea salt aerosol (SSA) is associated with open ocean sources such as wave breaking and bubble bursting (e.g.Nilsson et al. (2001)). However, SSA maxima have been observed in polar regions during winter and spring when the open ocean is furthest away (e.g. Sirois and Barrie (1999), Wagenbach et al. (1998)), and during glacial periods observed in ice core records (Wolff et al., 2003), and these maxima have not been captured in climate and aerosol models using exclusively open-ocean emissions as SSA sources (Huang and Jaeglé, 2017; Lapere et al., 2023). To account for this discrepancy, local sea ice sources of aerosol have been proposed. In particular, blowing snow events (BSEs), in which saline snow lofted during periods of high wind speeds sublimates and leaves behind impurities as aerosol, have been proposed as a significant local source of sea salt aerosol (Yang et al., 2008). Snow on sea ice acquires sea salt through a combination of the upward migration of brine from the sea ice surface, the integration of frost flowers to the bottom of the snowpack, and the advection and deposition of SSA from open ocean sources (Domine et al., 2004). In addition, snow on sea ice has been observed to contain extracellular polymeric

https://doi.org/10.5194/egusphere-2026-5047
Preprint. Discussion started: 26 August 2026

substances and bacteria in large quantities (Ewert et al., 2013), which may also be released into the atmosphere through the sublimation of surface snow. Research into blowing snow as a particle source has been motivated by modelling studies that included blowing snow as a ice aerosol source, and found an improved match between model simulations and SSA observations as a result (Levine et al., 2014; Huang and Jaeglé, 2017; Yang et al., 2019; Rhodes et al., 2017). The hypothesised production of SSA from blowing snow has subsequently recently been validated by direct observations in both the Arctic (Gong et al., 2023; Ranjithkumar et al., 2025; Bergner et al., 2025; Heutte et al., 2025) and the Antarctic (Frey et al., 2020). A synthesis of the current understanding of blowing snow over sea ice as a source of aerosol is included in Creamean et al. (2026).

The relevance of SSA from BSEs for both cloud properties and the polar energy budgets is not yet understood. The hygroscopicity of SSA allows it to act as an effective CCN (King et al., 2012), so that increases in SSA can lead to optically thicker clouds, which in turn can produce a surface warming effect in polar regions during winter and spring by trapping longwave radiation emitted at the surface. Gong et al. (2023) observed SSA production in the Central Arctic from BSEs concurrent to increases in CCNs, and calculated a resultant contribution to surface warming by SSA from BSEs of $+2.30\ \mathrm{Wm^{-2}}$ under cloudy conditions from November to April at latitudes north of $70°\mathrm{N}$. SSA has also been shown to act as an INP when combined with organic material (Alpert et al., 2022; DeMott et al., 2016), and surface snow may also contain additional INPs advected and deposited from regions beyond the sea ice, or from precipitation. The effect of BSEs on INPs has previously been addressed by Bergner et al. (2025), who observed concurrent increases in both SSA and CCNs during BSEs in the Central Arctic, and increases in INP concentrations at $-20\ °\mathrm{C}$ for 4 BSEs out of a total of 9 analysed, using the INP dataset presented in Creamean et al. (2022). However, they did not see a systematic relationship between INPs and BSEs across all BSEs observed.

In this paper, we investigate the relationship between BSEs and Arctic INPs in greater detail. We present year-round observations of INPs and major ions in the Central Arctic from October 2019 to October 2020, using filters taken during the MOSAiC campaign (Shupe et al., 2022), and improving upon the resolution measured in Creamean et al. (2022) from 3 days to 2 days. We performed INP analysis on samples of surface snow taken from the snowpack on sea ice and estimate their potential contribution to atmospheric INP concentrations. To constrain potential source contributions to INP populations, we assess the ion composition of filters taken at 1 week resolution, and of surface snow samples, and we compare these to those analysed from aerosol to assess the degree to which changes in aerosol compositions during BSEs can be attributed to the snow as a source. Finally, we present a series of case studies, and discuss the potential contributions to INPs during BSEs from both long-range transportation and the local sublimation of blowing snow.

2 Methods

2.1 Sample collection and preparation

All samples and data used in this paper were collected during the MOSAiC expedition, in which the research vessel (RV) *Polarstern* was frozen into Arctic sea ice and allowed to drift over the course of a year. MOSAiC began in September 2019, when RV Polarstern was frozen into sea ice located just north of the Laptev Sea, and allowed to passively drift along the Transpolar Drift Stream for most of the following 12 months, with a few transit periods. The drift and transit trajectories can

https://doi.org/10.5194/egusphere-2026-5047
Preprint. Discussion started: 26 August 2026

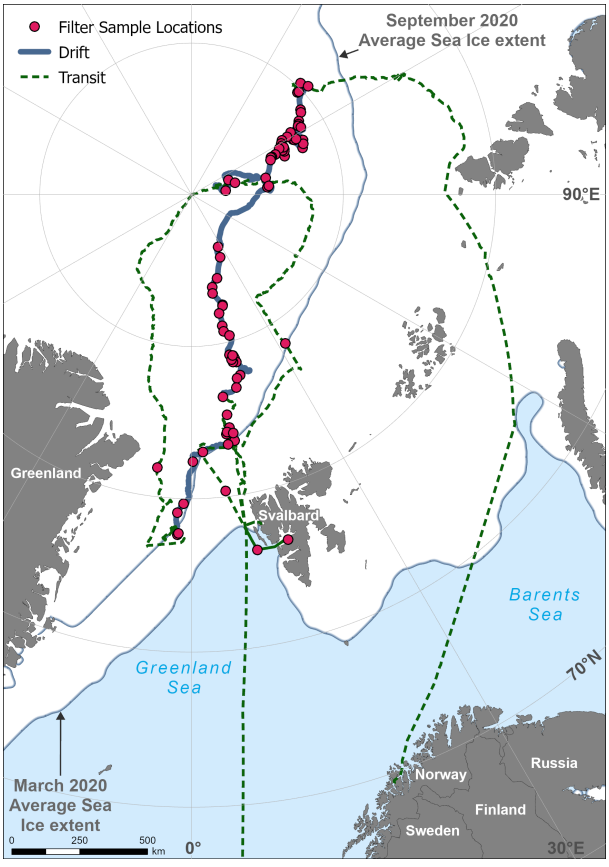

Figure 1. Map showing the MOSAiC trajectory, including both drift and transit periods. Air filter sampling sites are indicated at the coordinates corresponding to the median time during their 2-day filter exposure periods. Produced by the Mapping and Geographic Information Centre, British Antarctic Survey, 2026. Sea ice data taken from Fetterer et al. (2025)

be seen in Fig. 1. An overview of the MOSAiC journey and the atmospheric observations taken, including descriptions of Met City, the temporary atmospheric observatory station set up on the sea ice, can be found in Shupe et al. (2022).

Filter samples were collected at a 2-day resolution during MOSAiC, from 2 October 2019 to 3 October 2020. Track-etched polycarbonate filters (Whatman Nuclepore, 0.2 µm pore size, WHA111106) were used, which were cleaned using ultra-high-purity (UHP) water, microwaved for 2 minutes, and sonicated in an ultra-sonic bath for 10 minutes. The UHP water was then replaced and the filter was sonicated again. This step was repeated 4 times, left to soak overnight, and then sonicated again the following day. The filters were then dried in a desiccator, and packed into polythene bags, all in a class 100 cleanroom at the British Antarctic Survey (BAS) (Cambridge, United Kingdom). 16 samples were set aside and stored in the cleanroom to be used as procedural blanks. Samples were taken using an automatic filter sampler (Digitel DPA14 LoVol, Part-No. 13361) connected to a Total Suspended Particle (TSP) inlet in the BAS Atmospheric Container Laboratory, located at the bow of RV *Polarstern*, at approximately 10 m above the sea surface. The automatic sampler had a capacity of 30 filters, and once all filters

https://doi.org/10.5194/egusphere-2026-5047
Preprint. Discussion started: 26 August 2026

were used they were exchanged in a class 10 laminar flow hood. 186 filters were sampled in total, including 11 field blanks, which were sampled every 15 filters and were subjected to the pump running for 1 minute, but otherwise handled and processed identically to the samples. Typical volumes of sampled air from 2-day runs at standard temperature and pressure ($T = 0°C$, $p = 10^5$ Pa) were $50 - 60$ m^3 with an average flow rate of 18.56 L $\cdot$ min^{-1}, although some filters experienced significantly lower sampling times and yield volumes due to shutdowns from the pump reaching capacity. In particular, from 18 October to 19 November 2019, issues with frequent pump shutdowns resulted in the majority of filters being exposed to a reduced air volume, (average $V_{air} = 24.12$ m^3), which was frequently <50% of typical values of V_{air} for the rest of the year (average $V_{air} = 43.42$ m^3, median $V_{air} = 53.05$ m^3, excluding the pump shutdown period). 186 filters were taken in total, including 11 filters taken as field blanks. These field blanks were subjected to the pump running for 1 minute, but otherwise experienced identical storage and processing. The filters were packed and transported frozen at -20 °C for analysis at a laboratory at BAS. Measurement gaps exist during 2020 from the end of January to the start of March due a delay in the resupply of filters to the ship, from mid-April to early May due to a fault with the pump, and from mid-August to early September during a team transition period.

In total, a subset of 75 of the 2-day aerosol filters from a total of 186 were analysed to determine atmospheric INP concentrations as a function of activation temperature. For periods of time where filters were available, a filter from each week of MOSAiC was analysed, to get an understanding of the overall annual cycle. In addition, a higher density of filters during winter and spring were analysed to cover periods influenced by BSEs. A subset of 4 of the field blanks and 4 of the procedural blanks were also analysed. To prepare the filter samples for INP analysis, each filter was extracted using 4 ml of UHP water produced using an in-house Milli-Q system (Milli-Q Direct Water Purification System 8, Millipore) with a 0.2 µm end filter pore size, and a resistivity of 18.2 MΩ $\cdot$ cm at 25 °C. Each filter was shaken in UHP water for 20 minutes using a vortex mixer (Vortex-Genie 2, Scientific Industries), and removed after extraction. Some samples were extracted and processed for INP analysis on the same day, but when this was not possible, they were stored frozen at -20 °C.

Snow samples were taken from a series of centrally-organised snow pit sampling sites during MOSAiC to allow for the direct comparison of physical and chemical snow properties across a broad scope of analyses. Further information on snow sampling, the scope of analysis, and measurements sites can be found in Nicolaus et al. (2022) and Macfarlane et al. (2023). Snow was sampled at a 3 cm depth resolution, and stored frozen in 50 mL polypropylene tubes with screw caps (Corning CenriStar), which had been cleaned through rinsing with UHP water, and dried in a class 100 clean laboratory at BAS. 450 snow samples from a variety of depths across the entire year were analysed for major ion composition (Brown et al., 2025), with a subset of 59 surface samples analysed in this paper. 8 surface snow samples were analysed for INP concentration, representative of 1 week resolution each, and selected from November 2019 to April 2020 to cover periods affected by BSEs.

The size-resolved aerosol number concentration was measured using a Compact Lightweight Aerosol Spectrometer Probe (CLASP) at 2 m above the sea ice, at the NOAA meteorological tower mounted at the Met City site. The CLASP is a closed path optical spectrometer with a short 0.3 m intake tube designed to minimise particle loss to tube walls, and a 3 L $\cdot$ m^{-1} flow rate (Hill et al. (2008); Norris et al. (2008)). The CLASP measures aerosol number concentration across 16 size channels, spanning sizes $d_p = 0.5$ µm - 20 µm at ambient humidity, and has previously been used above Antarctic sea ice during winter

https://doi.org/10.5194/egusphere-2026-5047
Preprint. Discussion started: 26 August 2026

(Frey et al., 2020). Concentrations were initially measured at a rate of 10 Hz, but later averaged to 10 minute intervals. Further details on the NOAA meteorological tower can be found in Cox et al. (2023).

2.2 INP analysis

Temperature-resolved INP concentrations were measured using an offline immersion freezing droplet assay technique, based on the method described in Budke and Koop (2015), in which 1 µL-sized sample droplets are cooled down at a constant rate until freezing, and the temperatures at which they freeze are recorded. From the recorded freezing temperatures, temperature-resolved INP concentrations are then calculated using the method outlined in Vali (1971). Each INP is characterised by an activation temperature, and it is assumed that a droplet containing that INP freezes immediately after reaching the respective activation temperature. The concentration of INPs at a temperature T is given by:

$$[INP]_T = \frac{-ln(1 - f_{ice}(T))}{V_{droplet}} \cdot \frac{V_{wash}}{V_{air}} \tag{1}$$

where f_{ice} represents the frozen fraction of droplets at temperature T, $V_{droplet}$ represents the volume of the droplet, V_{wash} represents the volume of the UHP water used in extracting the filter, and V_{air} represents the volume of air drawn through the filter during collection. We report our INP concentrations at standard temperature and pressure.

Sample droplets were pipetted onto hydrophobic glass slides (Marienfeld, 0895040), and our method introduces a custom-built plastic spacer separating the droplets to prevent the Wegener–Bergeron–Findeisen process (Murphy and Koop, 2005). Images of the droplets were taken at a rate of $1\ \mathrm{s}^{-1}$ using a mounted camera (Microsoft Lifecam), and the detection of droplet freezing events was then automated from the visual contrast between liquid and frozen droplets in the images. All of the cold stage and sample preparation, including the pipetting of the samples and the cleaning of the glass slides with isopropanol (IPA, $> 99.5\%$ for HPLC, Thermoscientific) was carried out in a laminar flow hood (ISO Class 10 clean air conditions using HEPA filters, Monmouth Scientific).

For each run, 60 droplets were cooled down to $-35\ ^\circ\mathrm{C}$ at a rate of $1\ ^\circ\mathrm{C}$ per minute. A minimum of 2 runs per sample were implemented. If there was a significant deviation between the two runs identified through a quick visual inspection of their freezing spectra, a third run was implemented. A daily blank run consisting of 60 droplets of UHP water was analysed to monitor any drift in the background level of contamination. Despite mitigating efforts, freezing of UHP water almost always occurred at temperatures above homogeneous freezing (mean UHP freezing temperature $= -28.47\ ^\circ\mathrm{C}$, $\sigma = 2.67\ ^\circ\mathrm{C}$, homogeneous freezing temperature $\simeq -35^\circ\mathrm{C}$). This is due to the many potential sources of contamination and uncertainty from the freezing assay droplet method, including, but not limited to, droplet contact angle with the glass slides, laboratory environment, and even small particulate contaminants present in UHP water with diameters below the filter pore size ($< 0.2\ \mu\mathrm{m}$). Further discussion on the sources of systematic errors in droplet freezing experiments can be found in Polen et al. (2018).

When analysing INP concentrations from freezing droplet assay methods, and when comparing between methods and studies, we note that it is important to consider the upper and lower boundaries of the method resolution. This resolution is limited by the values of $V_{droplet}$, V_{wash}, V_{air}, and the number of droplets. Only one dilution ratio, R, was used for our samples, so

https://doi.org/10.5194/egusphere-2026-5047
Preprint. Discussion started: 26 August 2026

that

$$R = \frac{V_{wash}}{V_{droplet}} \tag{2}$$

This means that, for our method setup, for a median value of $V_{air} = 53.05\ \mathrm{m}^3$, the minimum resolvable INP concentration was $0.0013\ \mathrm{L}^{-1}$, and the maximum was $0.31\ \mathrm{L}^{-1}$, calculated using Eq. (1). In addition, if all of the activation temperatures of a sample are consistently warmer than the activation temperatures of the background, taken in this study to be the daily UHP water blank run, then we can infer that INP concentrations are high enough for saturation to have occurred. In droplet freezing experiments, saturation occurs when the number of INPs per droplet is high compared with the total number of droplets, so that all of the droplets freeze at warmer activation temperatures, and INPs active at colder temperatures go undetected. This results in an underestimation of reported INP concentrations, which worsens for colder activation temperatures, and cannot be quantified without further dilutions of each sample.

2.3 Ion chromatography

Ion chromatography analysis for major ion composition was implemented for weekly surface snow samples taken during MOSAiC. Each snow sample was melted, and an aliquot was taken and diluted using UHP water by at least a factor of 100 to keep the samples within the instrument calibration range. An ion chromatography system with reagent-free eluent generation (ICS-4000 Integrion) was used, with cation analysis implemented using an isocratic methylsulfonic acid elution through a CS12A separator column, and anion analysis implemented using a gradient elution with potassium hydroxide through an AS17 separator column. European reference materials ERM-CA408 for simulated rain water and CA616 for groundwater were analysed, and gave measurement accuracies within 5%.

Due to instrument malfunctions, it was not possible to perform the same analysis on the aerosol filter samples taken for INP analysis. Instead, we use an alternative dataset of major ion composition of filter samples with 1-week resolution taken from the roof of the BAS Atmospheric Container Laboratory during MOSAiC and analysed at the Atmospheric Chemistry Department (ACD) of the Leibniz Institute for Tropospheric Research (TROPOS) in Leipzig, as reported in Zeppenfeld et al. (2024). The ions discussed in this study are Na^+, Cl^-, NO_3^-, NH_4^+, Br^-, $CH_3SO_3^-$, and K^+.

2.4 Ancillary data

Blowing snow observations during MOSAiC were reported by Ranjithkumar et al. (2025), who characterised blowing snow events using a $10\ \mathrm{m}$ threshold wind speed $U_{t,10m}$, determined from the ambient temperature T_a and a minimum threshold wind speed of $U_{t0} = 6.9\ \mathrm{m \cdot s^{-1}}$ using an empirically-derived expression presented in Li and Pomeroy (1997), and a snow particle signal detected using an open path snow particle counter (SPC-95, Niigata Electric Co.,Ltd) (Nishimura et al. (2014); Frey et al. (2020)) mounted $0.08\ \mathrm{m}$ above the snow surface. Snow particle concentrations were measured in the size range of $36 < d_p < 490$ µm, and were also used in this study. From October 2019 to May 2020, 33 BSEs were detected, with an average duration of 2.16 days. The average $10\ \mathrm{m}$ wind speed during drifting and blowing snow was $U_{10m} = 7.6\ \mathrm{m \cdot s^{-1}}$, and the average ambient temperature at $2\ \mathrm{m}$ was $T_{2m} = -21.9\ ^\circ\mathrm{C}$ (Ranjithkumar et al., 2025). Due to the dependency of $U_{t,10m}$ on

https://doi.org/10.5194/egusphere-2026-5047
Preprint. Discussion started: 26 August 2026

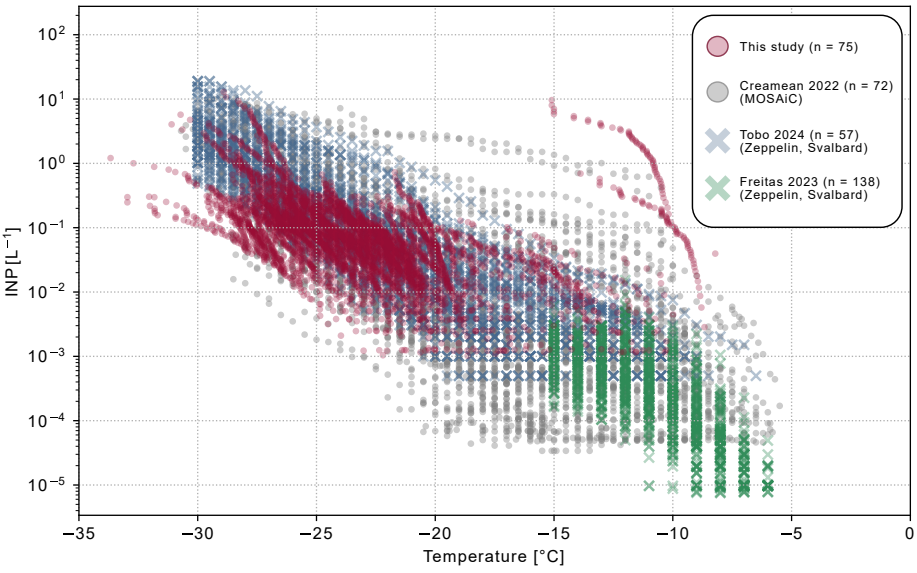

Figure 2. Atmospheric INP concentrations for 75 2-day aerosol filter samples taken during MOSAiC as a function of activation temperature. Filters were collected from 2 October 2019 to 3 October 2020. Three other INP studies have been plotted for comparison, showing INPs measured at Zeppelin Observatory (78.9 °N, 11.9 °E, 474 m above mean sea level) in Svalbard during a similar time period as MOSAiC (1 September 2019 to 3 October 2020) (Tobo et al., 2024), INPs also measured at Zeppelin Observatory for the period 5 January 2017 to 4 January 2020 (Freitas et al., 2023), and INPs observed from 3-day aerosol filters collected during MOSAiC (23 October 2019 to 1 October 2020) and analysed using an Ice Spectrometer (Creamean et al., 2022).

T_{2m}, and the reduced chance of a snow particle signal when $T_{2m} > 0$ °C and snow becomes too wet to become lofted by high wind speeds, no BSEs were detected during summer. Therefore, in this paper, we refer to the period encompassing October through May as the period affected by blowing snow events.

Additional meteorological data taken during MOSAiC were also used, with wind speed at 10 m, $U_{t,10m}$, and temperature at 2 m, T_{2m}, measured at the NOAA meteorological tower mounted at the Met City site, and accessed from Cox et al. (2023). Trajectory analyses from the FLEXPART model simulations, performed by the FLEXPART group at the University of Vienna, were also used (https://img.univie.ac.at/webdata/mosaic).

3 Results and discussion

3.1 Annual cycle of INPs

INP concentrations across all of the filters analysed can be seen in Fig. 2 (filters collected 2 October 2019 to 3 October 2020), and the fraction of droplets frozen prior to conversion to concentration can be seen in Fig. S1, alongside UHP blanks, procedural blanks, and field blanks. The majority of filters did not share activation temperatures with those observed in the

https://doi.org/10.5194/egusphere-2026-5047
Preprint. Discussion started: 26 August 2026

UHP background spectra, suggesting that our INP concentrations measured are underestimations, for the reasons discussed in Sect. 2.2. Further evidence for this underestimation comes from filters taken during the period of 18 October to 19 November 2019, during which, as discussed in Sect. 2.1, frequent pump shutdowns resulted in filters being exposed to lower air volumes. Despite this, freezing spectra significantly above background were still observed. As V_{air} is used to calculate atmospheric INP concentrations, the smaller values of V_{air} explain the larger values of INP concentrations calculated during this period in Fig. 4.

Our overall INP concentration spectra broadly agreed with similar studies, seeing significant overlap with INP data presented by Creamean et al. (2022) and Tobo et al. (2024) at activation temperatures below -20 °C. Creamean et al. (2022) investigated INPs using 3-day filter samples collected during MOSAiC and analysed using an Ice Spectrometer at Colorado State University. This method involved freezing larger sample volumes of 50 µL, allowing for an increased sensitivity to rarer INPs active at warmer temperatures. This accounts for the difference between this study's dataset and the results presented by Creamean et al. (2022) for INPs active at temperatures > -20 °C (Fig. 2). The dataset presented in Tobo et al. (2024) is the result of aerosol filters collected at 1-week resolution from 1 September 2019 to 3 October 2020, overlapping almost entirely with MOSAiC, but at Zeppelin Observatory (78.9 °N, 11.9 °E, 474 m above mean sea level) in Svalbard. This allows for a comparison with a terrestrial site in the Central Arctic. The samples were analysed in the immersion mode using the Cryogenic Refrigerator Applied to Freezing Test (CRAFT) system, using droplet volumes of $V = 5$ µL. Fig. 2 also shows INP concentrations collected at 1-week resolution from Zeppelin Observatory for the period 5 January 2017 to 4 January 2020, but analysed using a different technique, where 2 mm diameter holes were cut from the filters and immersed in UHP water (Freitas et al., 2023). This method was generally more sensitive to rarer INPs at warmer activation temperatures than the dataset in our study, but showed generally good agreement at temperatures where both studies were able to detect INPs (-15 °C $< T < -10$ °C).

In general, we observed a distinct seasonality of INPs, shown in the median activation temperatures for each sample in Fig. 3 and the concentrations of INPs at three activation temperatures (-15 °C, -20 °C, -25 °C) in Fig. 4. In summer, the number of sample droplets freezing at warmer temperatures increased. We measured INPs with activation temperatures ≥ -15 °C in 75% of samples during June, July, and August, compared with 19% of samples taken during October to May. The average INP concentration at -15 °C during summer was 0.49 L^{-1} ($N = 12$, $\sigma = 1.45$ L^{-1}), but this was significantly influenced by two consecutive filters in July with extremely enhanced INP concentrations above -15 °C, discussed further later in this section. Excluding these filters, the average INP concentration at -15 °C during summer was 0.016 L^{-1} ($N = 10$, $\sigma = 0.016$ L^{-1}). This is still an order of magnitude higher than INP concentrations at -15 °C for the rest of the year, during October to May, which averaged 0.0015 L^{-1} ($N = 58$, $\sigma = 0.0047$ L^{-1}). Similar summer peaks at -15 °C during MOSAiC were observed by Creamean et al. (2022), who reported that INPs active at temperatures ≥ -15 °C were the most abundant during June and July, and peaked at 0.02 L^{-1}, and at Zeppelin Observatory by Tobo et al. (2024), who saw average concentrations of 0.01 L^{-1} at -15 °C for June, July, and August, and also at studies conducted at Arctic terrestrial sites during other years (Wex et al., 2019; Sze et al., 2023). INP activity at temperatures greater than -15 °C has been seen in primary biological aerosol particles (PBAP), which are a subset of aerosol consisting of fragmented or intact biological cells (Pöschl et al., 2010; Hoose and Möhler, 2012), and can originate from both marine and terrestrial sources (Després et al., 2012). These warm INP Arctic

https://doi.org/10.5194/egusphere-2026-5047
Preprint. Discussion started: 26 August 2026

maxima have been linked specifically to local marine biological activity and PBAP through a number of avenues. Creamean et al. (2022) observed elevated chlorophyll-a, a marine primary producer proxy, during warm INP peaks, as well as an increase in the open water and melt pond fraction in the pack ice nearby. Barry et al. (2025) analysed aerosol filters from MOSAiC for bioaerosol, and used the presence of the marine-dwelling psychrophile *Polaribacter* as a tracer for local marine air masses, and the presence of fungi as a terrestrial tracer. They found an increase in the presence of both during summer INP peaks at -15 °C, indicating a mixed contribution in summer of both local marine sources and regional transport from terrestrial sources.

Two consecutive July filters (covering 25 July 2020, 15:03:29 UTC to 27 July 2020, 18:16:54 UTC) stand out in particular, with median activation temperatures of -11.27 °C and -13.24 °C, and elevated INP concentrations at -15 °C of 0.69 L^{-1} and 9.63 L^{-1}. These can be clearly seen in Fig. 2. The origins for air masses 24 hours prior to arriving at *Polarstern* for these filters based on the FLEXPART model simulations from the University of Vienna suggest a strong terrestrial influence from over Svalbard, and coarse aerosol concentrations during this period were heightened in general, with a median of 13.82 cm^{-3} for aerosol with $d_p = 0.5-20$ µm for the duration covering both filters, compared with a median of 2.84 cm^{-3} for July. Aerosol concentrations peaked at 18.64 cm^{-3} and 39.19 cm^{-3} for the two filters respectively, with the second filter experiencing the highest aerosol concentrations recorded by the CLASP during any filter sampling period across the entire campaign. INPs active at temperatures greater than -10 °C in the Arctic were detected by Creamean et al. (2022), and were observed to covary with hyperfluorescent aerosol, a tracer for PBAP, by Beck et al. (2024). However, these INPs were generally observed at lower concentrations than those observed in our two consecutive July filters. Tobo et al. (2024) also reported INP concentrations at Zeppelin Observatory in Svalbard for temperatures greater than -10 °C in early July, with the warmest freezing occurring at -5 °C and linked these to terrestrial sources of vegetation or dust from glacial outflow sediments that become local sources of INP in summer when surface air temperature rises above 0 °C and the proportion of snow-free surface increases. The uniqueness of these two filters in our dataset suggests that summertime terrestrial sources of warm temperature INPs from Svalbard rarely affect the aerosol population of the Central Arctic region over the sea ice.

During late autumn and early winter, median INP activation temperatures and concentrations were at their lowest. We observed the lowest INP concentrations across all temperatures selected (-15 °C, -20 °C, -25 °C) during November and December (Fig. 4). Some of the samples showed significant overlap with the UHP water background (Fig. S1), with 4 out of 17 samples during this time exhibiting median activation temperatures colder than 25% of the corresponding UHP blank activation temperatures. The only time that INPs were detected throughout November and December at activation temperatures > -20 °C was during a December storm, which is discussed further in Sect. 3.6. After 1 January 2020, INP concentrations rose to an average of 0.010 L^{-1} ($\sigma = 0.0068$ L^{-1}) at -20 °C during January, compared with an average of 0.0058 L^{-1} ($\sigma = 0.014$ L^{-1}) during December. This increase initially coincided with another storm, but INP concentrations at -20 °C remained elevated, compared with November and December, for the rest of the month. Arctic haze is a well-documented phenomenon in which Arctic aerosol concentrations dramatically rise in late winter and early spring due to the expansion of the polar front facilitating long-range transportation of pollution from lower latitudes (Shaw (1995)). During MOSAiC, Arctic haze arrived earlier than usual, with peaks in accumulation-mode aerosol and equivalent black carbon mass concentrations observed in January 2020, and attributed to an unusually strong positive phase of Arctic Oscillation (Boyer et al. (2023); Lawrence et al.

https://doi.org/10.5194/egusphere-2026-5047
Preprint. Discussion started: 26 August 2026

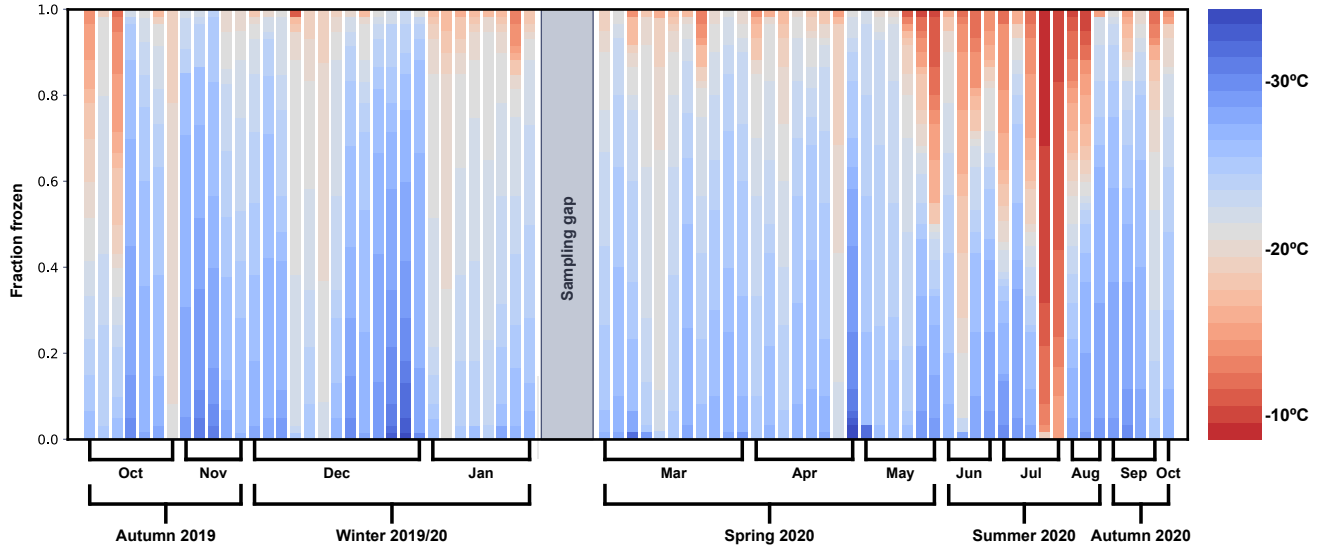

Figure 3. Fraction of droplets frozen during the immersion-mode freezing droplet assay method for 2-day aerosol filter samples colour-coded according to activation temperature.

(2020)). Increases in accumulation-mode aerosol from January onwards is also shown in Fig. 4.d, with lower concentrations observed in November and December, with the exception of the aforementioned December storm. Contrary to our results, the terrestrial study reported in Wex et al. (2019) found the lowest annual INP concentrations during the Arctic haze period, citing the poor ice nucleating properties of anthropogenic pollution found in Chen et al. (2018). In addition, Greenland ice core observations in Hartmann et al. (2019) showed that INP concentrations over the past 500 years did not increase in line with pollution tracers. It is likely that the increased INP concentrations at -20 °C that we observed during this time were not the direct result of anthropogenic pollution, but nonetheless still influenced by long-range transportation from terrestrial sources. Due to a sampling gap, mentioned in Sect. 2.1, INP measurements from February are unavailable. In spring, after measurements resumed on 2 March 2020, INPs during this time were characterised by concentrations at -20 °C averaging $0.14\ \mathrm{L}^{-1}$ ($N = 25$, $\sigma = 0.021\ \mathrm{L}^{-1}$) during March, April, and May. However, similar to late autumn and early winter, INPs at temperatures above -15 °C were rarely observed.

3.2 Atmospheric major ions and potential aerosol sources

The annual cycle of atmospheric major ions from filters taken with 1-week resolution gives context for our INP observations by providing insight into potential aerosol sources (Fig. 5, Fig. S2.a-e). In general, we observe three distinct periods in ion composition and concentration throughout the year. A summary of the key statistics for each ion observed for each period is shown in Table 1. The first period, from October 2019 until measurements paused in January 2020, is characterised by a large variability in concentrations for most ions, with the exception of Br^- and $CH_3SO_3^-$, which both exhibited minima during this

https://doi.org/10.5194/egusphere-2026-5047
Preprint. Discussion started: 26 August 2026

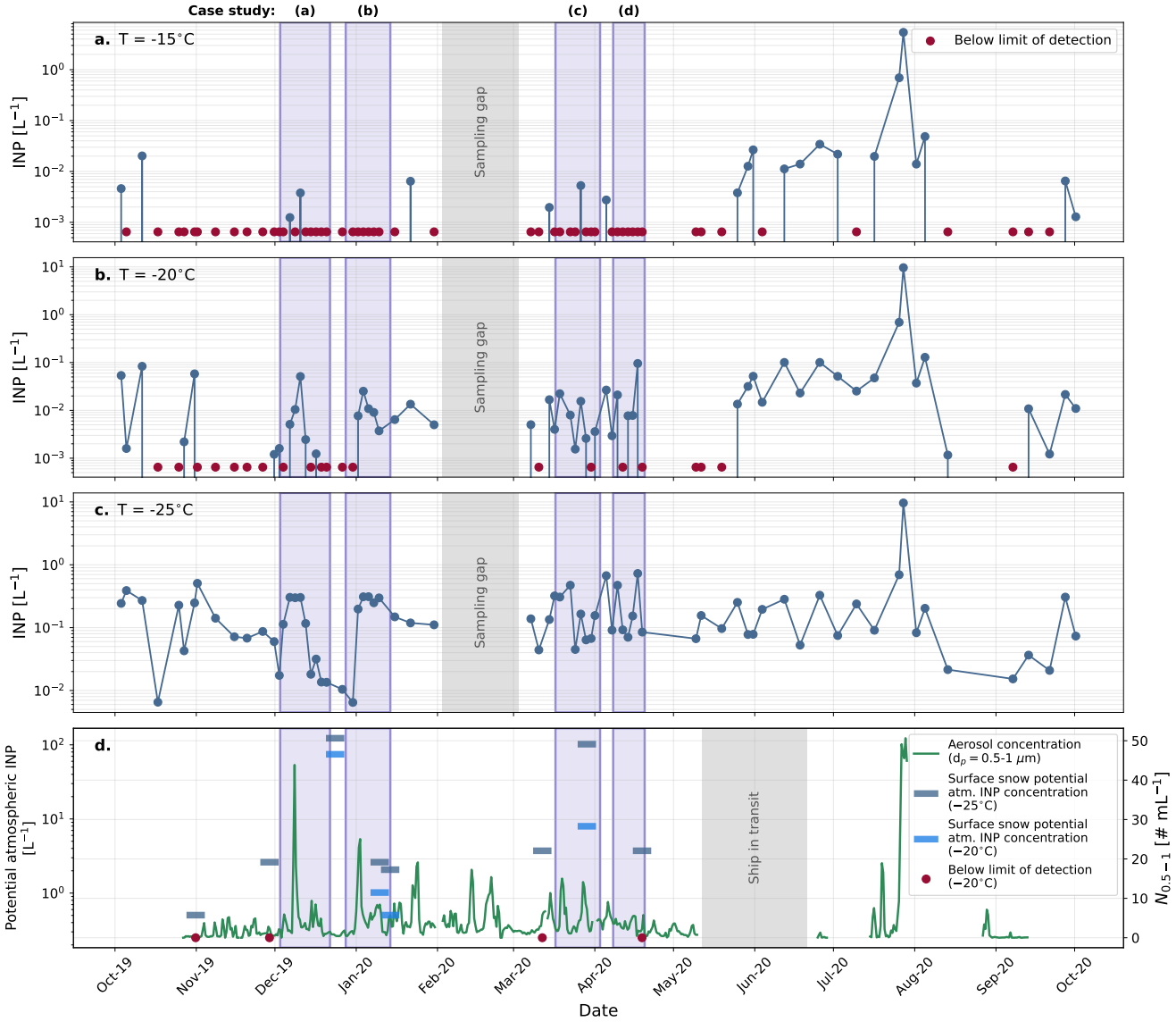

Figure 4. a - c show atmospheric INP concentrations for 2-day aerosol filter samples at three different temperatures. Filters for which no INPs were detected at that temperature have been indicated in red, and plotted at half the limit of detection (LOD). The LOD was calculated as the minimum resolvable INP concentration for the median value of V_{air}, as discussed in Sect. 2.2. The periods of time spanning the four case studies analysed in Sect. 3.6 are shown in purple, and the sampling gap due to a delay in the resupply of filters to the ship is shown in grey. The concentration of accumulation mode aerosol ($d_p = 0.5 - 1$ µm) measured using the CLASP is shown in d, alongside the potential atmospheric INP concentration measured from surface snow, at -20 °C and -25 °C, and shown by horizontal bars spanning the 7-week surface snow resolution. Potential atmospheric INP concentrations are calculated using the assumptions discussed in Sect. 3.4, and samples for which no INPs were detected at -20 °C are shown in red and plotted at half the LOD for potential atmospheric INP concentrations, which was taken as the minimum concentration calculated using the method outlined in Sect. 3.4. All snow samples exhibited INPs detected at -25 °C.

https://doi.org/10.5194/egusphere-2026-5047
Preprint. Discussion started: 26 August 2026

time. The second period, from March to May, is characterised by consistently high concentrations for the majority of ions, and lower variability compared with the first period. This period would have been heavily affected by Arctic haze, in which anthropogenic pollution drives the expected increase in SO_4^{2-}, NO_3^-, and NH_4^+, and the long-range transportation of K^+ from biomass burning, and Mg^{2+} and Ca^{2+} from terrestrial dust sources. Conversely, the concurrent peaks during this period in Na^+ and Cl^- are likely driven by local blowing snow (Huang and Jaeglé, 2017). The third period, from June to August, is characterised by high concentrations of $CH_3SO_3^-$, but low concentrations for most other ions, and suppressed variability in particular for Mg^{2+}, K^+, and Ca^{2+} compared with the first period. When comparing the percentage contributions of each ion to the total ion concentrations, we note that periods one and two shared similar percentage contributions despite the large difference in absolute ion concentrations (Fig. S3). The relative contributions shifted during period 3, during which $CH_3SO_3^-$ grew in significance from 0.9% to 4.7% , and Cl^- decreased in significance from 39.8% to 33.6% from period 2 to period 3. The decrease in significance of Cl^- during period 3 coincides with the end of the blowing snow season, as no blowing snow events were observed during period 3. The increase in significance of $CH_3SO_3^-$ during period 3 is indicative of an increase in local marine biogenic sources. In the aqueous phase, methanesulfonic acid (MSA) dissociates to methanesulfonate ($CH_3SO_3^-$), and so our reported concentrations of $CH_3SO_3^-$ are equivalent to concentrations of MSA. MSA is commonly used as a tracer for local marine biogenic sources due to the production of MSA from the oxidation of dimethyl sulfide (DMS), which is produced by phytoplankton near the ocean surface (Jongebloed et al., 2025).

To investigate the relative source contributions from sea-salt (ss) and non-sea-salt (nss) sources, nss-concentrations of Ca^{2+}, Mg^{2+}, and SO_4^{2-} were calculated using the following equation:

$$[ion]_{nss} = [ion]_{total} - [Na^+]_{total} \left(\frac{[ion]}{[Na^+]} \right)_{RSW} \quad (3)$$

where $[ion]_{nss}$ is the nss-concentration of an ion, $[ion]_{total}$ is the total concentration of that ion, and the ratio of the ion to Na^+ in reference seawater (RSW), taken from Millero et al. (2008), is used to scale for the sea-salt contribution. The proportions of sea-salt and non-sea-salt sources for Ca^{2+}, Mg^{2+}, and SO_4^{2-} for the three identified periods are shown in Fig. 5. During periods 1 and 2, Ca^{2+} and Mg^{2+} were predominately associated with sea-salt, with non-sea-salt contributions likely from continental dust. We observe similar relative contributions between periods 1 and 2 for sea-salt and non-sea-salt sources, but a significant increase in total ion concentrations during period 2 (table 1), shown in Fig. 6.a for nss-Ca^{2+} and nss-Mg^{2+}, and in Fig. 6.b. for nss-SO_4^{2-}, suggesting a comparable increase in both sea ice and open ocean sea-salt sources, continental dust sources, and anthropogenic pollution. Although the proportion of periods 1 and 2 affected by BSEs was very similar (24.6% of period 1 and 25.2% of period 2), it is possible that aerosol populations during period 2 were more affected by BSEs due to the increased sea ice coverage across the Arctic as a whole, which peaked during MOSAiC on 5 March 2020 (Perovich et al., 2020). However, period 2 also saw an increase in open lead fraction around *Polarstern* compared with period 1 (Krumpen et al., 2021), due to the ship drifting towards lower latitudes during this time. This could suggest that sea-salt aerosol release during BSEs has region-wide impacts on aerosol populations in the Central Arctic. The proportion of both Ca^{2+} and Mg^{2+} that were from nss sources compared with ss sources increased during period 3, indicating a greater importance of contributions from terrestrial dust sources. However, total concentrations of both nss and ss Ca^{2+} and Mg^{2+} decreased during period 3

https://doi.org/10.5194/egusphere-2026-5047
Preprint. Discussion started: 26 August 2026

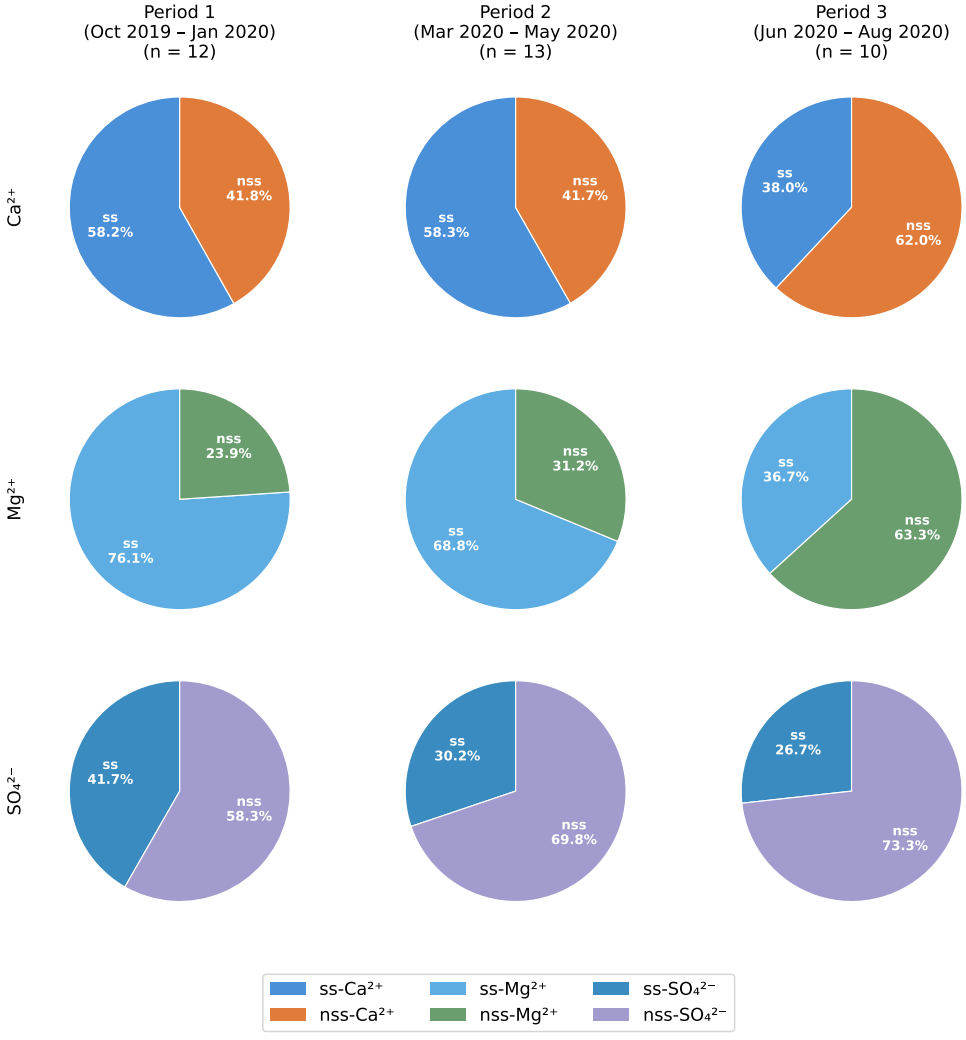

Figure 5. Relative contributions of sea-salt (ss) and non-sea-salt (nss) sourced ions for Ca^{2+}, Mg^{2+}, and SO_4^{2-} from 1-week filters during the three periods identified in Sect. 3.2.

https://doi.org/10.5194/egusphere-2026-5047
Preprint. Discussion started: 26 August 2026

Table 1. Mean and standard deviation for atmospheric concentrations of major ions in aerosol collected on filter samples at 1-week resolution. SO_4^{2-}, Ca^{2+}, and Mg^{2+} are split into total concentrations, and concentrations from non-sea-salt (nss) and sea-salt (ss) sources, calculated using Eq. (3). Period 1 covers October 2019 to January 2020, period 2 covers March 2020 to May 2020, and period 3 covers June 2020 to August 2020.

	Period 1 (mean $\pm\,\sigma$, ng $\cdot$ m^{-3}) ($n = 12$)	Period 2 (mean $\pm\,\sigma$, ng $\cdot$ m^{-3}) ($n = 13$)	Period 3 (mean $\pm\,\sigma$, ng $\cdot$ m^{-3}) ($n = 10$)
Na^+	255 ± 227	$1.28 \times 10^3 \pm 520$	307 ± 523
Cl^-	433 ± 419	$2.16 \times 10^3 \pm 1.14 \times 10^3$	456 ± 871
NO_3^-	30 ± 28.6	260 ± 114	19 ± 14
NH_4^+	21.1 ± 16.9	177 ± 94.1	61.5 ± 37.6
Br^-	4.53 ± 5.56	55.2 ± 84.6	1.95 ± 3.32
$CH_3SO_3^-$	0.279 ± 0.209	48.5 ± 45	63.6 ± 39
K^+	10.4 ± 11.2	48.1 ± 29.5	14.9 ± 22.1
SO_4^{2-} (total)	148 ± 136	$1.07 \times 10^3 \pm 355$	289 ± 208
SO_4^{2-} (ss)	61.7 ± 52.2	322 ± 131	77.3 ± 132
SO_4^{2-} (nss)	86.2 ± 111	745 ± 344	212 ± 151
Ca^{2+} (total)	16.7 ± 13.9	83.1 ± 42.5	30.9 ± 43
Ca^{2+} (ss)	9.7 ± 8.72	48.4 ± 19.9	11.7 ± 20
Ca^{2+} (nss)	6.98 ± 7.74	34.7 ± 27.8	19.1 ± 31.8
Mg^{2+} (total)	38.6 ± 43	217 ± 137	93 ± 197
Mg^{2+} (ss)	29.3 ± 27.8	149 ± 64.6	34.2 ± 63.3
Mg^{2+} (nss)	9.24 ± 24.6	67.8 ± 83.9	58.9 ± 176

compared with period 2, suggesting that, whilst ss-Ca^{2+} and ss-Mg^{2+} both decrease after the end of the blowing snow season as expected, aerosol concentrations attributed to terrestrial dust sources also decrease, indicating a reduction in contributions from long-range transportation.

SO_4^{2-} was predominately nss sourced across all three periods, with the lowest nss contribution in period 1, and comparable nss contributions in periods 2 and 3. The increase in nss-SO_4^{2-} contributions, alongside increases an absolute concentrations, in period 2 is indicative of the influence of Arctic haze, involving the transportation of anthropogenic SO_4^{2-} released from industrial processes at lower latitudes. The proportion of nss-SO_4^{2-} is maintained through to period 3, whilst absolute concentrations decrease. We observed an increased correlation between nss-SO_4^{2-} and $CH_3SO_3^-$ in period 3 ($R^2 = 0.39$, $p = 0.0542$) (Fig. 7) whilst we observed no correlation during period 2, indicating that, whilst the proportion of nss-SO_4^{2-} is similar between periods 2 and 3, the sources of nss-SO_4^{2-} shift from anthropogenic emissions to biogenic sources.

https://doi.org/10.5194/egusphere-2026-5047
Preprint. Discussion started: 26 August 2026

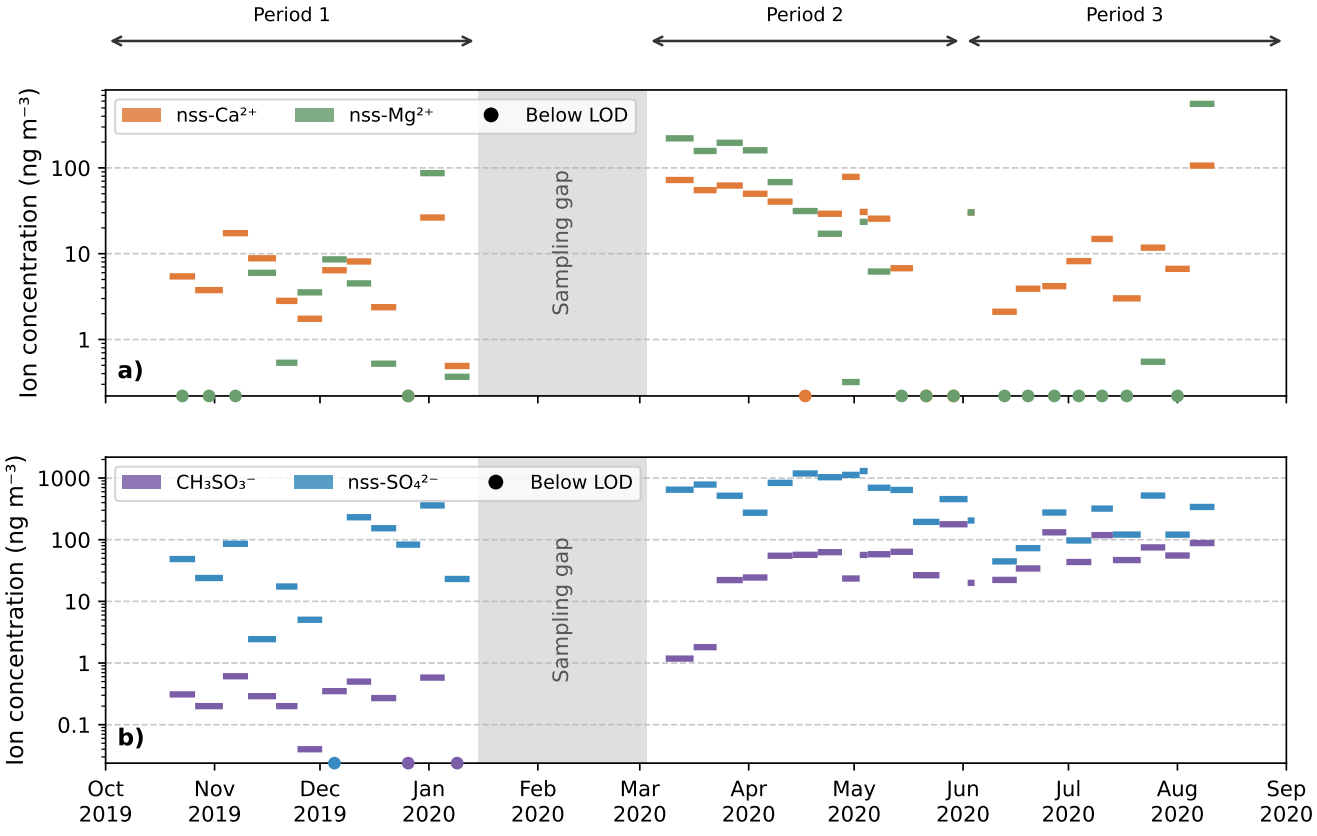

Figure 6. Atmospheric concentrations of major ions in aerosol collected on filter samples at 1-week resolution. The width of each horizontal bar represents the sampling duration of the filter. Plot a) shows the concentrations of nss-Ca^{2+} and nss-Mg^{2+}, and plot b) shows nss-SO_4^{2-}, with $CH_3SO_3^-$ plotted alongside as a tracer for marine biogenic sources of aerosol. The sampling gap due to a delay in the resupply of filters to the ship is shown in grey. Samples for which the calculated nss contribution was negative are plotted as dots on the x-axis, and treated as below the LOD.

345 The three periods observed throughout the year for major ions align with the variability observed in our INP annual cycle in Fig. 3. During the first period, we observed low activation temperatures occurring in late autumn and early winter (mean $T_a = -24.39$ °C, $\sigma = 3.58$ °C from October 2020 to December 2020), alongside low INP concentrations at temperatures above our detection limit (median INP concentration from October 2020 to December 2020 at -20 °C $= 0.011$ L^{-1}) . The high variability displayed by the ion concentrations is also reflected by the multiple filters exhibiting spuriously warmer activation
350 temperatures observed during this period. During the second period, INP concentrations at -20 °C were consistently elevated compared to the first period (Fig. 4.b.), echoing the high concentrations and low variability exhibited by most ions during this time. It is possible that the increases in INP concentrations at -20 °C are partially driven by increases in continental dust sources during this time, with peaks in nss-Ca^{2+} and nss-Mg^{2+} during March (Fig. 6). In summer, INP concentrations above

https://doi.org/10.5194/egusphere-2026-5047
Preprint. Discussion started: 26 August 2026

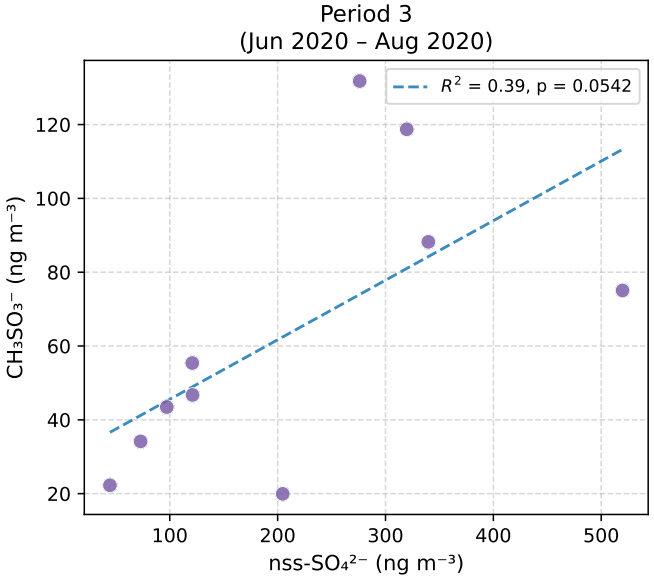

Figure 7. Concentrations of $CH_3SO_3^-$ versus nss-SO_4^{2-} for period 3 identified in Sect. 3.2. A line of best fit is shown using blue dotted lines, with $R^2 = 0.39$ and $p = 0.0542$. No correlation was observed for periods 1 or 2.

-15 °C peaked, despite lower ion concentrations, but coinciding with a maxima in $CH_3SO_3^-$, and an increased contribution from biogenic nss-SO_4^{2-}, further enforcing the attribution of these warm INPs to local marine biogenic sources. Although $CH_3SO_3^-$ concentrations were also reasonably high during spring, in period 2, the majority of filters sampled during the same period did not exhibit INP concentrations above -15 °C, and we observed no correlation between $CH_3SO_3^-$ and nss-SO_4^{2-}.

Each filter at 1-week resolution was compared with the periods affected by BSEs to determine how much each filter overlapped with blowing snow. Major ion concentrations as a function of the overlap with BSEs can be seen in Fig. S4. Statistically significant ($p < 0.05$) positive correlations between ion concentrations and overlap with blowing snow periods were observed for Cl^- ($R^2 = 0.23$, $p = 0.017$), K^+ ($R^2 = 0.32$, $p = 0.004$), and Mg^{2+} ($R^2 = 0.27$, $p = 0.009$). We did not observe a statistically significant dependence of ion concentration on blowing snow overlap for the remainder of our ions, although we note that Na^+ was close to the threshold ($R^2 = 0.14$, $p = 0.076$). When we grouped our filters into those with $< 20\%$ overlap with BSEs and those with $\geq 20\%$ overlap, we also observed an increase in the percentage contribution to total ion concentration of Cl^- from 34.0% to 45.5%, and of Na^+ from 22.7% to 24.8% (Fig. S5). We expect increases in Cl^- and Na^+ during BSEs, as strong correlations between BSEs and NaCl peaks have previously been observed in multiple blowing snow studies at higher temporal resolution (< 30 minutes) (Gong et al., 2023; Bergner et al., 2025), or inferred from sodium concentrations (Frey et al., 2020). This justifies our use of this ion dataset at a comparatively coarser temporal resolution to investigate the impact of BSEs on atmospheric ion concentrations.

In summary, we find three periods of distinct ion composition, which align with variation observed in our INP data. By using MSA and nss- and ss- Mg^{2+}, Ca^{2+}, and SO_4^{2-} as aerosol source tracers, we find that aerosol populations, and potentially INPs,

https://doi.org/10.5194/egusphere-2026-5047
Preprint. Discussion started: 26 August 2026

during period 2 were strongly influenced by simultaneous increases in aerosol from both BSEs and long-range transportation. We also find that elevated INP concentrations and activation temperatures during period 3 were driven by regional biogenic sources, based on the positive correlation between MSA and nss-SO_4^{2-}. Due to the similarity in percentage contributions from nss- and ss- sources between periods 1 and 2, it is still an open question as to what degree increases in INP concentrations from period 1 to period 2 are driven by BSEs or long-range transportation.

3.3 Comparisons with ions in surface snow

To investigate the impact of surface snow as a source of aerosol, we compare ion concentrations in surface snow with ion concentrations in the atmosphere using the enrichment of each ion relative to RSW, with Na^+ as the reference ion. An enrichment factor f was calculated for each ion, so that:

$$f = \frac{k}{k'} \tag{4}$$

where

$$k = \left(\frac{[ion]}{[Na^+]}\right)_{sample}, k' = \left(\frac{[ion]}{[Na^+]}\right)_{RSW} \tag{5}$$

so that k is the mass ratio of the ion to Na^+ in the sample, and k' is the mass ratio of the ion to Na^+ in RSW. These ratios can be seen in Fig. 8 for samples collected during the blowing snow season (October 2019 to May 2020). Statistically significant shifts of f during BSEs (samples with $\geq 20\%$ overlap with BSEs) occurred for Cl^-, SO_4^{2-}, and K^+, according to Wilcoxon rank-sum tests ($p < 0.05$). In general, Cl^- was slightly depleted in both aerosol and snow relative to RSW, with BSEs minimizing this depletion further. The depletion of Cl^- in aerosol outside of BSEs (median $f = 0.86$) was very similar to the depletion found in surface snow (median $f = 0.87$), whereas f during BSEs (median $f = 0.96$) was statistically significantly different from surface snow ($p = 0.0123$). This weak increase in f of Cl^- associated with BSEs is therefore indicative of a non-local effect, such as long-range transportation associated with storm activity during blowing snow events. However, the opposite effect was observed for K^+, with f representing a depletion for aerosol outside of BSEs (median $f = 0.76$), and a mild enrichment both during BSEs (median $f = 1.15$) and surface snow (median $f = 1.04$), suggesting contributions to aerosol species from sublimating snow during BSEs.

SO_4^{2-} was enriched in aerosol relative to RSW, (median $f = 3.97$), but this enrichment was diminished during BSEs (median $f = 2.74$), whilst surface snow on average showed little enrichment of SO_4^{2-} (median $f = 1.09$), but displayed a large variation encompassing both significant enrichment and depletion. In general, we expect enrichment of SO_4^{2-} in aerosol during the blowing snow season, and particularly in spring, due to the transportation of anthropogenic SO_4^{2-} during Arctic haze from industrial centres. Heutte et al. (2025) found the highest monthly median mass concentrations of SO_4^{2-} during MOSAiC in April, coinciding with when Boyer et al. (2023) found a large influence on aerosol populations from transport from Siberia. Heutte et al. (2025) also found elevated SO_4^{2-} during two storm case studies encompassing blowing snow events, during November 2019 and March 2020. This appears to contradict the decreased enrichment of SO_4^{2-} during blowing snow events (Fig. 8).

https://doi.org/10.5194/egusphere-2026-5047
Preprint. Discussion started: 26 August 2026

However, Heutte et al. (2025) also observed a decoupling of SO_4^{2-} peaks and wind speed peaks, alongside a high correlation between SO_4^{2-} and equivalent black carbon concentrations, therefore arguing that the increased SO_4^{2-} during the blowing snow events was due to concurrent long range transportation, rather than from local sublimating blowing snow. Depletion of SO_4^{2-} in surface snow can be explained by the precipitation of mirabilite (Frey et al., 2020), which competes in the Arctic with the effect of anthropogenic sulfate, resulting in the large spread of both enrichment and depletion of SO_4^{2-} observed in surface snow (Fig. 8). This suggests that, whilst long range transportation may have produced SO_4^{2-} peaks during blowing snow case studies presented by Heutte et al. (2025), blowing snow itself has a depleting effect on SO_4^{2-} in aerosol due to the comparatively lower ratios of SO_4^{2-}:Na^+ in surface snow.

We did not observe a statistically significant impact on the enrichment factors of Mg^{2+}, Br^-, or Ca^{2+} by BSEs. For Br^-, this is unsurprising, as seasonal changes in atmospheric bromine concentrations in the Arctic are strongly influenced by springtime bromine explosion events, driven by heterogeneous reactions on sea ice, snow, and aerosol surfaces during sunlit periods (Richter et al., 1998; Fan and Jacob, 1992). However, we did observe a sizeable increase in the median values of f for Br^- (median $f = 1.46$ for samples with $< 20\%$ overlap with BSEs, median $f = 3.04$ for samples with $\geq 20\%$ overlap with BSEs), with BSEs bringing aerosol enrichment of Br^- closer to that found in surface snow (median $f = 3.38$). This is in line with model studies identifying blowing snow as a source of atmospheric bromine (Yang et al., 2008; Marelle et al., 2021), due to heterogeneous reactions on SSA released through blowing snow. Frey et al. (2020) observed strong enrichment of Br^- in Antarctica for aerosol at 2 m above the sea ice surface, and depletion at 29 m. They concluded that SSA from blowing snow constitutes a bromine reservoir that significantly depletes between 2 m and 29 m above the sea ice surface. Unlike the results from this study, they did not observe overall enrichment in the snowpack, although they acknowledge a large scatter of enrichment and depletion across their snowpack samples. However, Yang et al. (2024) observed significant Br^- enhancements in surface snow at a coastal Arctic site, using data collected at both on-shore and off-shore sampling locations. For Mg^{2+} and Ca^{2+}, the lack of a statistically significant change in f during BSEs is likely due to the fact that the enrichment factors observed in filters outside of BSEs already showed similar values to those found in snow for these ions.

Overall, we observe a complicated relationship across the ions measured between atmospheric and surface snow composition. Previous work on aerosol increases during BSEs have emphasised sublimating snow as a source of SSA (Gong et al., 2023; Frey et al., 2020). However, changes in SSA concentrations have no impact on enrichment factors. Therefore, the shift in enrichment factors observed for Cl^-, SO_4^{2-}, and K+ towards values found in surface snow are indicative of a non-SSA contribution from surface snow to aerosol composition during BSEs. Our results also suggest that the effect of blowing snow on aerosol chemical composition is driven by a combination of local emission from sublimating snow, and concurrent long-range transportation, and is likely strongly case-dependant. This is investigated further through a series of case studies in Sect. 3.6.

3.4 INPs in surface snow

We saw a large variability in INP concentrations and activation temperatures across surface snow samples taken from November 2019 to April 2020 (Fig. 9.a and Fig. 4.d.). Five of our samples exhibited median activation temperatures between -25 °C and -30 °C, and overlapped with the coldest observed activation temperatures for the filters, as well as some overlap with

https://doi.org/10.5194/egusphere-2026-5047
Preprint. Discussion started: 26 August 2026

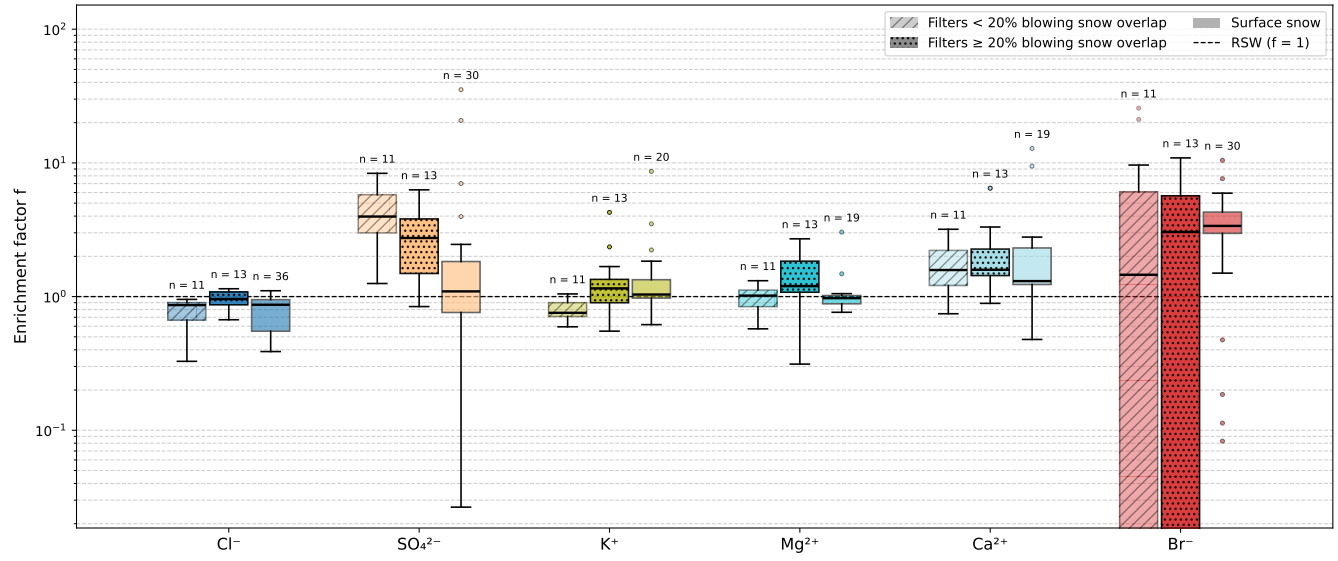

Figure 8. Enrichment factor f of major ions relative to Na^+ with respect to RSW for filter samples with $< 20\%$ overlap with BSEs, for filter samples with $\geq 20\%$ overlap with BSEs, and for surface snow samples. Filter and snow samples are restricted to those collected during the blowing snow season (October 2019 to May 2020). For each box plot, the box boundaries span the interquartile range (IQR), and the median is given by the black horizontal line. The whiskers indicate the most extreme data point within the range spanning $1.5 \cdot$ IQR, and any data points outside of this are shown as circular markers.

the two UHP water background runs observed on the days these samples were analysed. One surface snow sample had very low activation temperatures, with a median activation temperature of $-31.08\ ^\circ\mathrm{C}$. Two surface snow samples showed elevated activation temperatures. The sample taken on 1 March 2020 had a median activation temperature of $-21.19\ ^\circ\mathrm{C}$, and overlapped consistently with the warmer activation temperatures observed in the filters. The sample taken on 27 December 2019 stands out the most, with a median activation temperature of $-15.26\ ^\circ\mathrm{C}$. These two samples demonstrate a potential diversity of INPs present in surface snow.

To assess the potential impact of INPs measured in the surface snow on atmospheric INP populations during blowing snow events, we converted the INP concentration in the melted snow samples to potential atmospheric INPs. We assumed a snow density of $0.3\ \mathrm{g \cdot cm^{-3}}$, and that the top $0.1\ \mathrm{cm}$ of snow entirely sublimates during a blowing snow event, releasing all of the INPs contained in that layer, which are then distributed throughout a boundary layer height of $230\ \mathrm{m}$. To justify these assumptions, we refer to Cheng et al. (2025), who reported a mean snow density of $0.283 \pm 77\ \mathrm{g \cdot cm^{-3}}$ from surface snow samples collected during MOSAiC from October 2019 to May 2020, and to Peng et al. (2023), who reported a mean atmospheric boundary layer height during MOSAiC of $231\ \mathrm{m}$. We also refer to Robinson et al. (2025), who reported a mean blowing snow sublimation flux of $0.014\ \mathrm{cm \cdot SWE \cdot day^{-1}}$ during MOSAiC from 1 November 2019 to 1 May 2020. For a mean snow density of $0.3\ \mathrm{g \cdot cm^{-3}}$ and an average blowing snow duration of 2.16 days, this translates to a mean blowing

https://doi.org/10.5194/egusphere-2026-5047
Preprint. Discussion started: 26 August 2026

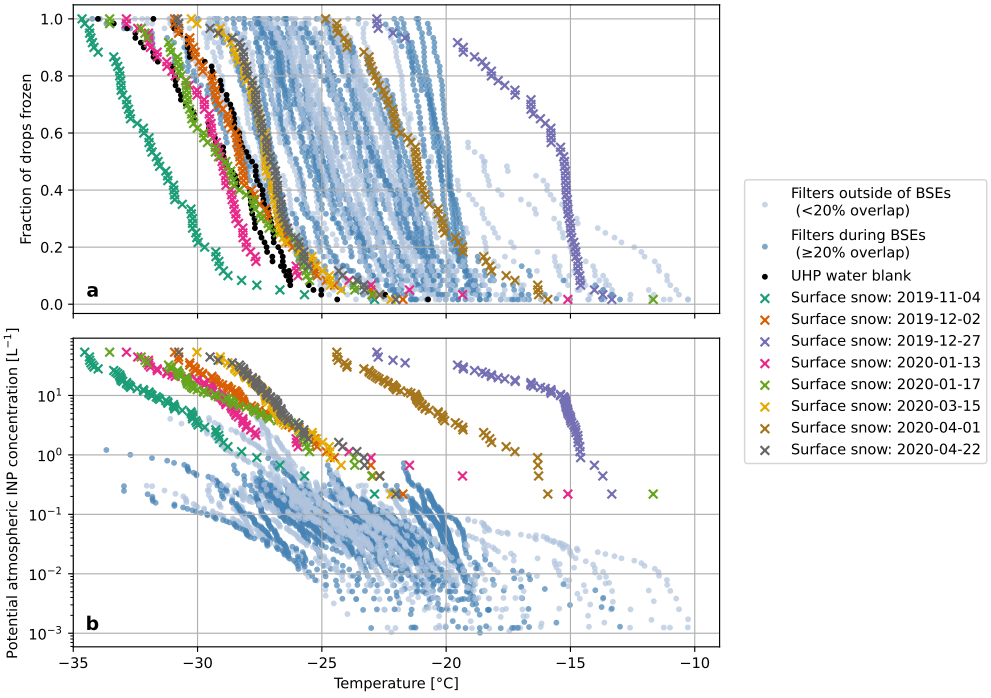

Figure 9. Plot (a) shows the fraction of droplets frozen for surface snow and filter samples as a function of activation temperature. Surface snow samples are plotted using X markers, and filter samples during the blowing snow period (October 2019 to May 2020) are plotted with blue dots, with darker dots indicating filters with $\geq 20\%$ overlap with BSEs, and lighter dots indicating filter samples with $< 20\%$ overlap with BSEs. The two UHP water blank samples corresponding to the days where the surface snow samples were analysed are plotted in black. Plot (b) shows the potential atmospheric INP concentrations from snow samples, calculated assuming the sublimation of the top 0.1 cm of surface snow, alongside atmospheric INP concentrations calculated from the filters.

snow sublimation flux of 0.1 cm of snow per BSE. Figure 9.b. shows the resultant potential atmospheric INP concentrations from surface snow plotted alongside the atmospheric INP concentrations measured from filter samples. Potential atmospheric INP concentrations from surface snow consistently showed similar or greater concentrations of INPs at equivalent activation temperatures below -23 °C than the atmospheric INP concentrations from filters, with the two surface snow samples with elevated activation temperatures exhibiting INP concentrations 1 to 2 orders of magnitude greater than those seen in all of the filters at all activation temperatures, excepting the filter taken on 27 July 2020, discussed in Sect.3.1.

3.5 The impact of blowing snow events

When comparing filters during BSEs and filters outside of BSEs for the period in which we observed blowing snow (October 2019 to May 2020), we saw no statistically significant effect ($p < 0.05$) on INP concentrations for activation temperatures at or above -20 °C and -25 °C, based on a Wilcoxon rank-sum test. This is shown in Fig. 10.a. We defined filters during BSEs

https://doi.org/10.5194/egusphere-2026-5047
Preprint. Discussion started: 26 August 2026

as those with $\geq 20\%$ overlap between the sampling time period and BSE time periods. Our results are consistent with those reported by Bergner et al. (2025), who found no statistically significant difference in INP concentrations at $-15°C$ for filters intersecting with BSEs.

However, we note that presenting INP concentrations at selected activation temperatures results in a loss of information, as filters will only appear to differ if their freezing spectra differ *over* the selected activation temperature. Since the majority of our filters were subject to similar air volumes, except for those discussed in Sect. 2.1 and taken during 18 October to 19 November 2019, and to identical laboratory analysis, it is valid to compare their freezing properties amongst the sample set prior to using Eq. (1) for the conversion to concentration. As shown in Fig. 10.b., filters that overlapped with BSEs exhibited warmer median droplet activation temperatures, which increased by an average of 0.78 °C for samples with a $> 25\%$ overlap, 1.33 °C for samples with a $> 50\%$ overlap, and 1.66 °C for samples with a $> 75\%$ overlap. This change is not significant enough to be reflected in the comparisons between INP concentrations in Fig. 10.a, especially since the droplet freezing spectra of samples do not always differ around the temperatures selected for comparisons (-20 °C and -25 °C in Fig. 10.a), but nonetheless this 'warm shift' indicates a change in atmospheric INPs associated with BSEs. Although we observed an increase in median activation temperatures for all three overlap percentages presented in Fig. 10.b, which increased with increasing overlap, Wilcoxon rank-sum tests performed between the populations during BSEs and outside BSEs did not suggest statistical significance ($p < 0.05$). It is possible that this increase in activation temperature is the product of noise; however, we note the presence of distinct warm shifts in multiple blowing snow case studies, discussed later in Sect. 3.6, and shifts in activation temperatures would also have been influenced by the seasonal changes noted in Sect. 3.1.

Increases in the median activation temperature with BSEs is surprising, as the INPs measured in the surface snow samples in Sect. 3.4 typically exhibited colder or similar activation temperatures to those measured from the filters, barring two exceptions. However, this increase is consistent with the surface snow as an INP source. If the underlying types of INPs remain the same (i.e. a constant probability density function of activation temperatures), but total INP concentrations increase significantly, then we would also see a shift to warmer median activation temperatures as the likelihood of a sample droplet containing an INP active at warmer temperatures increases, and INPs active at colder temperatures in the same droplet go undetected. de Almeida Ribeiro et al. (2023) tested the sensitivity of the freezing spectra derived from droplet-freezing experiments to the number of droplets used per sample, and the range of dilutions of the sample tested. They showed that, for droplet experiments with limited sampling (100 droplets per sample), if the lowest resolvable dilution (number of INPs per droplet $= 1$) is not tested, then the estimation of the underlying distribution of activation temperatures becomes poor, and the median activation temperature detected can increase by at least 0.5 °C, as colder INPs go undetected. If we assume that total INP concentrations scale with total aerosol concentrations, then we can see this impact in the weak but statistically significant positive correlation ($R^2 = 0.217$, p-value $p = 0.001$) between aerosol concentration for $d_p = 0.5 - 20$ µm, and median droplet activation temperature (Fig. S6). Because of the impact that increased INP concentrations have on the results of droplet freezing experiments, moderate warm shifts in activation temperatures without significant changes in reported concentrations at selected activation temperatures are compatible with an INP source that has a similar activation temperature distribution as the baseline INP distri-

https://doi.org/10.5194/egusphere-2026-5047
Preprint. Discussion started: 26 August 2026

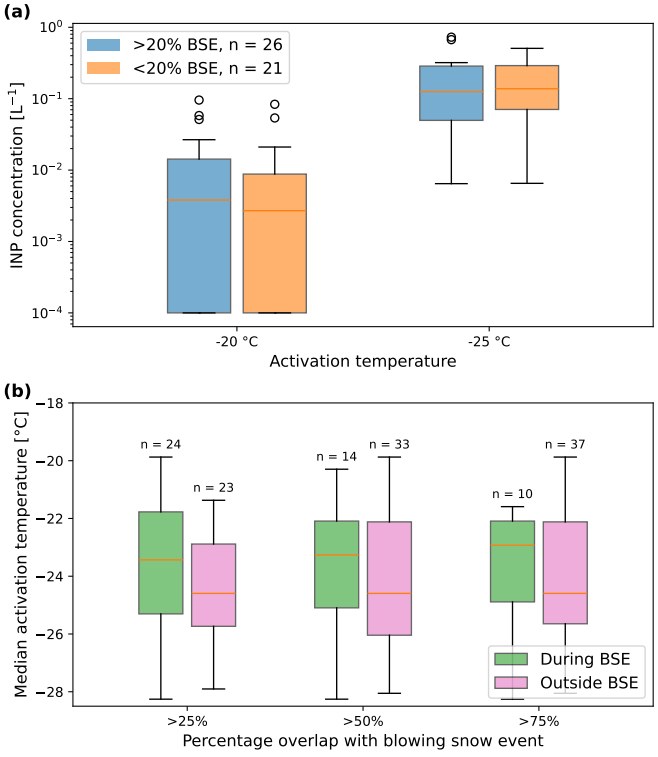

Figure 10. Plot (a) shows box plots comparing INP concentrations at -20 °C and -25 °C, for events with a $\geq 20\%$ temporal overlap with BSEs shown in blue, and with a $< 20\%$ temporal overlap shown in orange. To allow for plotting on a logarithmic scale, zero values have been replaced by 10^{-4} L^{-1}. Plot (b) shows box plots of the median activation temperatures for INPs during and outside of BSEs, for three different percentage overlaps that each sample has with BSEs ($> 25\%$, $> 50\%$, and $> 75\%$). For each box plot, the box boundaries span the interquartile range (IQR), and the median is given by the orange horizontal line. The whiskers indicate the most extreme data point within the range spanning $1.5 \cdot$ IQR, and any data points outside of this are shown as circular markers.

bution. This means that small increases in median activation temperatures observed in filters during BSEs are consistent with, but not evidence for, sublimating surface snow during BSEs as a local source of INPs.

3.6 Case studies

To better understand the relationship between increases in activation temperatures and total aerosol during BSEs, four case studies were selected to encompass both BSEs and background periods, to reflect seasonal diversity, and to maximise the temporal density of filters available. Each case study contains at least one notable aerosol peak associated with a BSE. Median aerosol concentrations for $d_p = 0.5-20$ µm were 1.8 cm^{-3} during the period of 15 October 2019 to 9 May 2020 (Ranjithkumar et al. (2025)), and all four of the most significant aerosol peaks in each case study in Fig. 11 show aerosol concentration increases of at least an order of magnitude from this baseline, with concentrations of a) 20.93 cm^{-3}, b) 13.80 cm^{-3}, c) 13.03

https://doi.org/10.5194/egusphere-2026-5047
Preprint. Discussion started: 26 August 2026

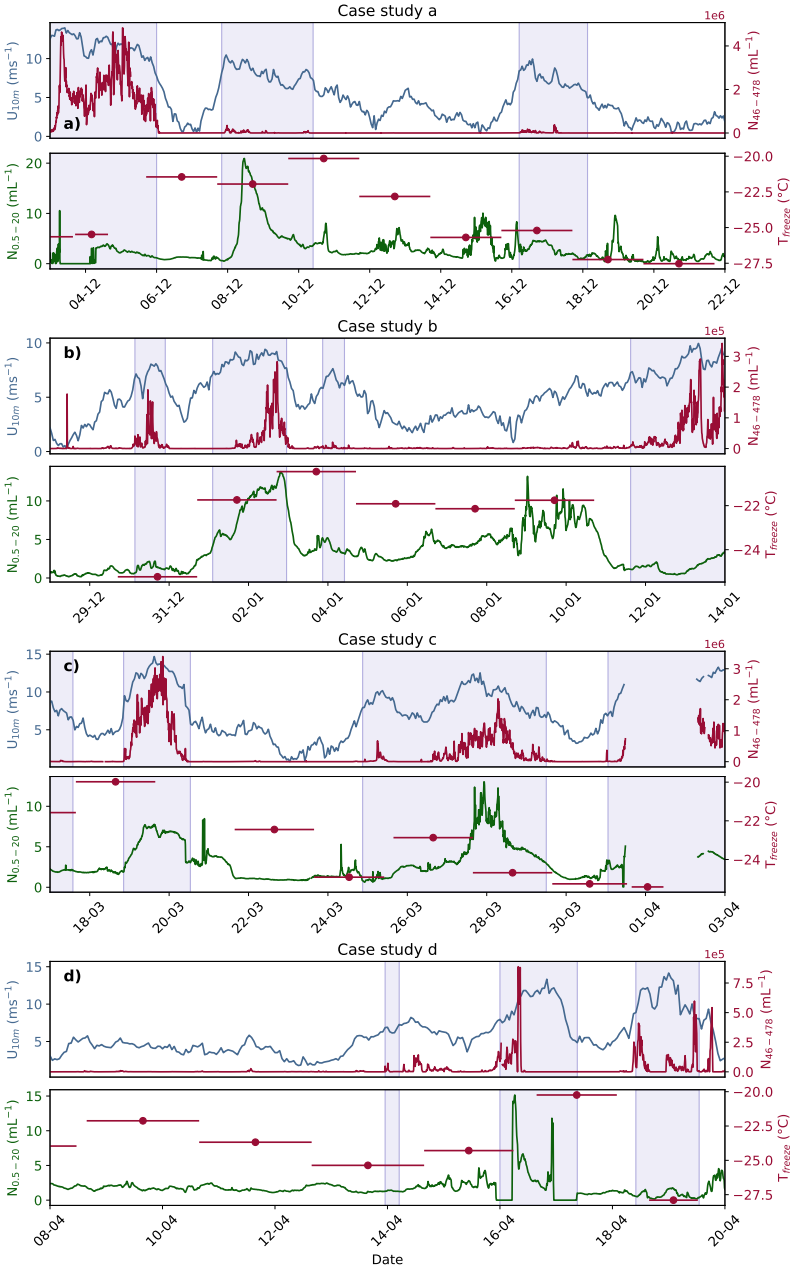

Figure 11. Four case studies selected during MOSAiC. For each case study, the upper plot shows 10 m wind speed, U_{10m}, and 0.08 m snow particle concentration for diameters $d_p = 46-478$ µm, N_{46-478}, and the lower plot shows aerosol number concentration for diameters $d_p = 0.5-20$ µm, $N_{0.5-20}$, and median activation temperatures for each aerosol filter sample analysed using the droplet assay method, T_{freeze}. BSEs are indicated in the purple shaded areas.

https://doi.org/10.5194/egusphere-2026-5047
Preprint. Discussion started: 26 August 2026

cm^{-3} and d) 15.15 cm^{-3}. For case studies a, b, and d, the most significant aerosol peaks were all immediately followed by the INP filter with the warmest median activation temperature, T_{freeze}, throughout the case study. This pattern was not observed in case study c. In addition, case studies a and b encompass blowing snow events also investigated in Bergner et al. (2025), who observed enhanced INP concentrations at -20 °C for 10 November 2019 to 12 November 2019, and for 7 December 2019 to 10 December 2019.

To differentiate between possible source contributions to the INPs in each case study, we investigated the ion concentrations for the filters encompassing the aerosol peak for each case study. These were compared against the average concentrations of each ion for the corresponding background period excluding BSEs, identified in Sect. 3.2 as the three distinct periods in ion concentrations observed throughout the year. For case studies a and b, this was period 1 (October 2019 to January 2020) and for case studies c and d this was period 2 (March 2020 to May 2020). The concentrations and relative changes for notable ions, as well as the time periods for each case study, ion filter, and background period, can be seen in Fig. 12. We also differentiated the four case studies by their 7-day air parcel histories, which varied significantly throughout, but did all include some Eurasian terrestrial influence (Fig. S7).

From the ion concentrations presented (Fig. 12), we determine that case studies a, b, and c all experienced contributions from both long-range transportation and local blowing snow to their aerosol composition. We use increases in Na^+ and Cl^- as indicators of sublimating snow as an aerosol source, nss-Ca^{2+} and nss-Mg^{2+} as tracers for terrestrial dust, and nss-SO_4^{2-} as a tracer for anthropogenic pollution. Case studies a, b, and c experienced sizeable increases in Na^+ and Cl^-, with Na^+ increasing by a) 91.1%, b) 68.0%, and c) 39.0% from the respective background periods. This indicates that sublimating blowing snow was a significant aerosol contributor during these three case studies. Case study b showed extremely large increases in nss-Ca^{2+} (278%), nss-Mg^{2+} (840%), and nss-SO_4^{2-} (318%) compared with the background period (Fig. 12.b), suggesting influences from both terrestrial dust sources, and anthropogenic pollution, alongside a strong contribution to air parcel history from northern Russia (Fig. S7.b). Gong et al. (2023) investigated a similar period to case study a, and reported elevated concentrations of black carbon during the BSE coinciding with the INP warm shift, indicating the influence of aerosol from long-range transportation of biomass-burning plumes. This is also demonstrated in the elevated nss-SO_4^{2-} (168% increase from the background concentration) observed during this time (Fig. 12.a).

Case study d did not show significant changes in Na^+ or Cl^- for the filter encompassing its aerosol peak, suggesting low contributions from SSA, and therefore low contributions from blowing snow. However, the aerosol peak in case study d has previously been extensively linked to long-range transportation, as it coincided with a warm air mass intrusion (WAMI) event, during which pollutants from industrial centres in Northern Eurasia experienced anomalous transportation to the location of *Polarstern*. This event is extensively documented in Dada et al. (2022), and involved an air temperature increase from -30.8 °C to -3.1 °C over a 2 day period. Particle concentrations also increased drastically, with the measurement site temporarily experiencing concentrations in the size range $d_p < 1$ µm equivalent to mid-latitudes. Barry et al. (2025) reported increased INP concentrations at -15 °C during the April WAMI at the location of *Polarstern*, as well as the presence of fungi in the bioaerosol population, which they used as a tracer for terrestrial origins of air masses and were not present in samples taken before or after the WAMI. We observed enhanced concentrations of nss-SO_4^{2-} which, during period 2, was primarily

https://doi.org/10.5194/egusphere-2026-5047
Preprint. Discussion started: 26 August 2026

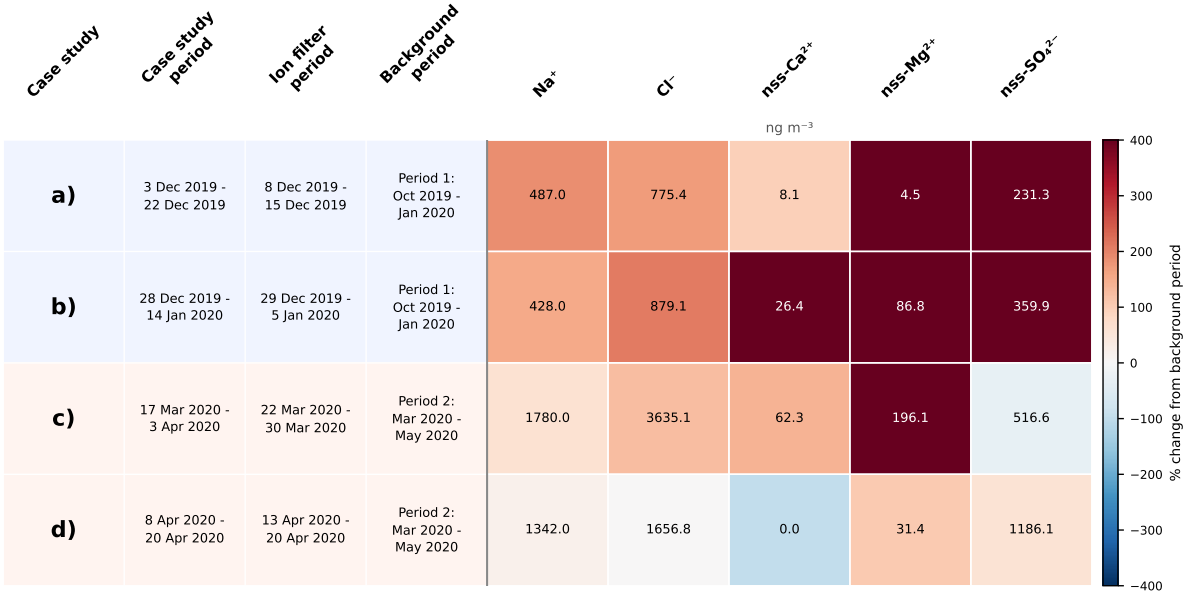

Figure 12. Ion concentrations from filters of 1-week resolution. For each case study, a filter was selected that sampled the time period encompassing the aerosol peaks observed during the case studies a, b, c, and d (Fig. 11). The colour of each cell represents the percentage change in ion concentration for that filter compared with the average ion concentration during the background period. The background periods were identified in Sect. 3.2.

associated with anthropogenic pollution, but decreased concentrations of nss-Ca^{2+} and nss-Mg^{2+}, suggesting that this case study was likely not affected by terrestrial dust sources (Fig. 12.d). We conclude that the INP warm shift associated with case study d is attributable to long-range transportation, and not to sublimating blowing snow.

Case study c is the only case study to not show an INP warm shift associated with a blowing snow aerosol peak, and is also the only case study to show a decrease in the concentration of nss-SO_4^{2-}, compared with the background period (Fig. 12.c). As discussed in Sect. 3.3, we observed on average a decrease in the enrichment of nss-SO_4^{2-} for filters affected by blowing snow events across the whole of MOSAiC, approaching the lower enrichment values observed in surface snow on sea ice. This may indicate that, of the four case studies, case study c is the most representative of aerosol sources dominated by blowing snow, suggesting that blowing snow itself may not be the main contributor to the increase in activation temperatures associated with BSEs.

4 Conclusions

Unravelling the impact of sublimating blowing snow as a source of INPs from the impact of long-range transportation is complicated. Previous work has demonstrated BSEs to be a significant source of sea-salt aerosol (Gong et al., 2023; Ranjithkumar et al., 2025; Bergner et al., 2025; Heutte et al., 2025; Frey et al., 2020), and found no clear relationship between INP concen-

https://doi.org/10.5194/egusphere-2026-5047
Preprint. Discussion started: 26 August 2026

trations calculated from offline methods and BSEs (Bergner et al., 2025). In this work, using INP and major ion concentrations measured from filters and surface snow, we present evidence for BSEs as a source of non-sea-salt aerosol, and argue that our results are compatible with BSEs as a source of INPs.

We observed a connection between the ion composition of surface snow and aerosol during blowing snow events. Blowing snow events had a statistically significant depleting effect for aerosol on SO_4^{2-}, and a statistically significant enriching effect on Cl^- and K^+. For SO_4^{2-}, K^+, and Br^-, blowing snow events brought the enrichment factors of these ions with respect to Na^+ closer to the values found in surface snow, indicating that the sublimation of snow is a source of non-sea-salt associated ions. We also observed INPs in surface snow active at temperatures similar to those observed in aerosol, especially at colder activation temperatures ($T < -23$ °C). An estimation of potential atmospheric INP concentrations from the sublimation of surface snow using a simple model suggested that the INPs observed in surface snow were present at concentrations significant enough to account for observed atmospheric INP concentrations. This is a crude model, and ignores any removal of INPs from deposition, but it demonstrates the potential of surface snow as a reservoir of INPs at concentrations significant for atmospheric INP populations.

Although INP concentrations at activation temperatures of -20 °C and -25 °C were unaffected by blowing snow events, as also observed in Bergner et al. (2025), we did see an increase in median activation temperatures of 1.66 °C for samples that overlapped with blowing snow events for at least 75% of their sampling duration. Although this increase was not statistically significant, when we analysed a series of 4 blowing snow case studies we observed increases in median activation temperatures associated with aerosol peaks during blowing snow events for 3 of the case studies. We argue that these small activation temperature increases are consistent with an increase in INP concentrations during BSEs at activation temperatures similar or lower than those observed in aerosol during baseline periods. We also argue that such an increase would not impact our reported INP concentrations at -20 °C and -25 °C due to the limitations of the droplet freezing assay method. However, we also found evidence for influences of long-range transportation during BSEs using tracers of dust and anthropogenic aerosol, as we observed increases in non-sea-salt sourced Ca^{2+}, Mg^{2+}, and SO_4^{2-} during case studies, and simultaneous increases in aerosol sourced from BSEs and long-range transportation during March, April, and May, preventing us from attributing changes in INP concentrations during this time to either source. We also observed a lack of increase in INP activation temperatures for 1 case study with ion composition that suggested that, of the 4 case studies observed, this one had the most significant influence from blowing snow.

In addition to our evaluation of the impact of BSEs on Arctic aerosol populations, we also report on the seasonal cycle of INPs and major ions in the Central Arctic, finding good agreement with previous Arctic INP studies (Creamean et al., 2022; Tobo et al., 2024). INPs exhibit a strong seasonal cycle, with significantly enhanced INP concentrations at -15 °C in the summer months, low INP concentrations at -20 °C and colder activation temperatures during late autumn and early winter, and sustained concentrations at -20 °C during spring. This generally followed the annual trend also observed in atmospheric ion concentrations, which was characterised by three distinct periods. By using MSA as a tracer for biogenic marine sources of aerosol, INP peaks at warm activation temperatures in summer were linked to local open-ocean sources. The low ice nucleation activity in late autumn and early winter followed trends of suppressed concentrations across most ions measured, suggesting

https://doi.org/10.5194/egusphere-2026-5047
Preprint. Discussion started: 26 August 2026

that INP concentrations in the Central Arctic track general changes in the strength of various aerosol sources, including both BSEs and long-range transportation. In addition, in this work we show that the correlation between MSA and nss-SO_4^{2-} in summer, and lack of correlation elsewhere, indicated a shift from high levels of anthropogenic sulfate in spring, to high levels of biogenic sulfate in summer. Finally, although we observed high concentrations of INPs at warm activation temperatures ($T > -15$ °C) for two samples associated with summertime terrestrial aerosol sources from Svalbard, we conclude that the uniqueness of these two samples in our dataset indicate that these sources from Svalbard do not influence the rest of the central Arctic region.

We conclude that, whilst the ion compositions measured suggest a snow-atmosphere connection during BSEs beyond previously reported emissions of SSA, and whilst BSEs did increase the median activation temperatures of INPs, it is not clear that this impact on INPs are the result of sublimating blowing snow. INP observations with a higher temporal resolution are required to better constrain the relationship between INPs and blowing snow events. In particular, higher resolution studies are required to investigate the degree to which sublimation and deposition drive the connection between atmospheric and surface snow INP populations. To further understand the mechanisms causing shifts in INP activation temperatures during BSEs in future, and resultant climate implications of this potential particle source in an otherwise remote region, we recommend online methods, such as the Portable Ice Nucleation Experiment (PINE) (Möhler et al., 2021), or the SPectrometer for Ice Nuclei (SPIN) (Garimella et al., 2016).

Data availability. The filter and surface snow INP data, and major ion concentrations in surface snow will be made available, and respective DOIs are forthcoming. Major ion concentrations in filters with 1-week resolution can be found via the World Data Centre PANGAEA (https://doi.org/10.1594/PANGAEA.973882, Zeppenfeld et al. (2024)). MOSAiC meteorological data is available via the Arctic Data Center (https://arcticdata.io/catalog/view/doi%3A10.18739%2FA2PV6B83F , Cox et al. (2023)). MOSAiC snow particle number densities and aerosol particle number densities measured using the CLASP are available via Zenodo (https://doi.org/10.5281/zenodo.13760111, Ranjithkumar (2024)).

Author contributions. MMF planned and performed data and sample collection during MOSAiC. The laboratory method for INP analysis was set-up and developed by FvdH, with contributions from MMF and MM, and INP analysis was performed by MM and MMF. Ion chromatography analysis of major ion concentration of MOSAiC snow samples was performed by SM and MMF, and ion chromatography analysis of major ion concentration of MOSAiC filter samples was performed by MvP and SZ. MM performed the scientific analysis presented in the manuscript, with contributing guidance from MMF, FvdH, XY, and RR. MM wrote the manuscript with contributions from all co-authors.

Competing interests. All authors declare that they have no competing interests.

https://doi.org/10.5194/egusphere-2026-5047
Preprint. Discussion started: 26 August 2026

Acknowledgements. This research has been made possible through the financial support of the Natural Environment Research Council (UK) through both the funding of the studentship of MM through the C-CLEAR DTP (grant number NE/S007164/1) and the SSAASI-CLIM project to MMF (grant number NE/S00257X/1). In addition, we gratefully acknowledge the funding by the Deutsche Forschungsgemeinschaft (DFG, German Research Foundation) - Project number 268020496 - TRR 172, within the framework of the Transregional Collaborative Research Center 'ArctiC Amplification: Climate Relevant Atmospheric and SurfaCe Processes, and Feedback Mechanisms (AC)^3'. Data used in this manuscript originates from field work carried out as part of the international Multidisciplinary drifting Observatory for the Study of Arctic Climate (MOSAiC) with the tag MOSAiC20192020. We thank all persons involved in the expedition of the RV *Polarstern* during MOSAiC in 2019–2020 (AWI PS122 00) as listed in Nixdorf et al. (2021). We are grateful for instrument support to ensure continuous year-round sampling during MOSAiC, in particular to Amélie Kirchgäβner, Matthew Shupe, Taneil Uttaal, Laurianne Quélévere, Ivo Beck, and Tuija Jokinen. We are thankful also to Ian Brooks for providing the CLASP instrument and support.

https://doi.org/10.5194/egusphere-2026-5047
Preprint. Discussion started: 26 August 2026

References

Albrecht, B. A.: Aerosols, Cloud Microphysics, and Fractional Cloudiness, Science, 245, 1227–1230, https://doi.org/10.1126/science.245.4923.1227, 1989.

Alpert, P. A., Kilthau, W. P., O'Brien, R. E., Moffet, R. C., Gilles, M. K., Wang, B., Laskin, A., Aller, J. Y., and Knopf, D. A.: Ice-nucleating agents in sea spray aerosol identified and quantified with a holistic multimodal freezing model, Science Advances, 8, eabq6842, https://doi.org/10.1126/sciadv.abq6842, 2022.

Barry, K. R., Hill, T. C. J., Kreidenweis, S. M., DeMott, P. J., Tobo, Y., and Creamean, J. M.: Bioaerosols as indicators of central Arctic ice nucleating particle sources, Atmospheric Chemistry and Physics, 25, 11 919–11 933, https://doi.org/10.5194/acp-25-11919-2025, 2025.

Beck, I., Moallemi, A., Heutte, B., Pernov, J. B., Bergner, N., Rolo, M., Quéléver, L. L. J., Laurila, T., Boyer, M., Jokinen, T., Angot, H., Hoppe, C. J. M., Müller, O., Creamean, J., Frey, M. M., Freitas, G., Zinke, J., Salter, M., Zieger, P., Mirrielees, J. A., Kempf, H. E., Ault, A. P., Pratt, K. A., Gysel-Beer, M., Henning, S., Tatzelt, C., and Schmale, J.: Characteristics and sources of fluorescent aerosols in the central Arctic Ocean, Elementa: Science of the Anthropocene, 12, 00 125, https://doi.org/10.1525/elementa.2023.00125, 2024.

Bergner, N., Heutte, B., Beck, I., Pernov, J. B., Angot, H., Arnold, S. R., Boyer, M., Creamean, J. M., Engelmann, R., Frey, M. M., Gong, X., Henning, S., James, T., Jokinen, T., Jozef, G., Kulmala, M., Laurila, T., Lonardi, M., Macfarlane, A. R., Matrosov, S. Y., Mirrielees, J. A., Petäjä, T., Pratt, K. A., Quéléver, L. L. J., Schneebeli, M., Uin, J., Wang, J., and Schmale, J.: Characteristics and effects of aerosols during blowing snow events in the central Arctic, Elementa: Science of the Anthropocene, 13, 00 047, https://doi.org/10.1525/elementa.2024.00047, 2025.

Boyer, M., Aliaga, D., Pernov, J. B., Angot, H., Quéléver, L. L. J., Dada, L., Heutte, B., Dall'Osto, M., Beddows, D. C. S., Brasseur, Z., Beck, I., Bucci, S., Duetsch, M., Stohl, A., Laurila, T., Asmi, E., Massling, A., Thomas, D. C., Nøjgaard, J. K., Chan, T., Sharma, S., Tunved, P., Krejci, R., Hansson, H. C., Bianchi, F., Lehtipalo, K., Wiedensohler, A., Weinhold, K., Kulmala, M., Petäjä, T., Sipilä, M., Schmale, J., and Jokinen, T.: A full year of aerosol size distribution data from the central Arctic under an extreme positive Arctic Oscillation: insights from the Multidisciplinary drifting Observatory for the Study of Arctic Climate (MOSAiC) expedition, Atmospheric Chemistry and Physics, 23, 389–415, https://doi.org/10.5194/acp-23-389-2023, 2023.

Brown, L. V., Pound, R. J., Jones, M. R., Rowlinson, M. J., Chance, R., Jacobi, H.-W., Frey, M. M., Archer, S. D., Arndt, S., Barten, J. G. M., Blomquist, B. W., Dadic, R., Ganzeveld, L. N., Hannula, H.-R., Helmig, D., Jaggi, M., Krampe, D., Macfarlane, A. R., Miller, S., Schneebeli, M., and Carpenter, L. J.: Iodine speciation in snow during the MOSAiC expedition and its implications for Arctic iodine emissions, Faraday Discuss., 258, 441–472, https://doi.org/10.1039/D4FD00178H, 2025.

Budke, C. and Koop, T.: BINARY: an optical freezing array for assessing temperature and time dependence of heterogeneous ice nucleation, Atmospheric Measurement Techniques, 8, 689–703, https://doi.org/10.5194/amt-8-689-2015, 2015.

Chen, J., Wu, Z., Augustin-Bauditz, S., Grawe, S., Hartmann, M., Pei, X., Liu, Z., Ji, D., and Wex, H.: Ice-nucleating particle concentrations unaffected by urban air pollution in Beijing, China, Atmospheric Chemistry and Physics, 18, 3523–3539, https://doi.org/10.5194/acp-18-3523-2018, 2018.

Cheng, Y., Cheng, B., Pirazzini, R., Macfarlane, A. R., Vihma, T., Dorn, W., Dadic, R., Schneebeli, M., Arndt, S., and Rinke, A.: Seasonal evolution of snow density and its impact on thermal regime of sea ice during the MOSAiC expedition, The Cryosphere, 19, 6001–6021, https://doi.org/10.5194/tc-19-6001-2025, 2025.

Cox, C., Gallagher, M., Shupe, M., Persson, O., Blomquist, B., Grachev, A., Riihimaki, L., Kutchenreiter, M., Morris, V., Solomon, A., Brooks, I., Costa, D., Gottas, D., Hutchings, J., Osborn, J., Morris, S., Preusser, A., and Uttal, T.: Met City Meteorological and Surface

https://doi.org/10.5194/egusphere-2026-5047
Preprint. Discussion started: 26 August 2026

Flux Measurements (Level 3 Final), Multidisciplinary Drifting Observatory for the Study of Arctic Climate (MOSAiC), Central Arctic, October 2019 - September 2020, https://doi.org/10.18739/A2PV6B83F, 2023.

Creamean, J., Barry, K., and et al., T. H.: Annual cycle observations of aerosols capable of ice formation in central Arctic clouds, Nature Communications, 13, 2022.

Creamean, J. M., Miller, L. A., van Pinxteren, M., Crabeck, O., Steiner, N. S., Marelle, L., Deschepper, I., Lapere, R., León-Marcos, A., Pratt, K. A., Thomas, J. L., Da Silva, A., Frey, M. M., Peeken, I., Horowitz, H. M., Willis, M. D., and Price, R.: Polar primary aerosols across the ocean-sea ice-snow-atmosphere interface: From sources to impacts, Elementa: Science of the Anthropocene, 14, 00 065, https://doi.org/10.1525/elementa.2025.00065, 2026.

Dada, L., Angot, H., Beck, I., et al.: A central Arctic extreme aerosol event triggered by a warm air-mass intrusion, Nature Communications, 13, 5290, https://doi.org/10.1038/s41467-022-32872-2, 2022.

de Almeida Ribeiro, I., Meister, K., and Molinero, V.: HUB: a method to model and extract the distribution of ice nucleation temperatures from drop-freezing experiments, Atmospheric Chemistry and Physics, 23, 5623–5639, https://doi.org/10.5194/acp-23-5623-2023, 2023.

DeMott, P. J., Hill, T. C. J., McCluskey, C. S., Prather, K. A., Collins, D. B., Sullivan, R. C., Ruppel, M. J., Mason, R. H., Irish, V. E., Lee, T., Hwang, C. Y., Rhee, T. S., Snider, J. R., McMeeking, G. R., Dhaniyala, S., Lewis, E. R., Wentzell, J. J. B., Abbatt, J., Lee, C., Sultana, C. M., Ault, A. P., Axson, J. L., Martinez, M. D., Venero, I., Santos-Figueroa, G., Stokes, M. D., Deane, G. B., Mayol-Bracero, O. L., Grassian, V. H., Bertram, T. H., Bertram, A. K., Moffett, B. F., and Franc, G. D.: Sea spray aerosol as a unique source of ice nucleating particles, Proceedings of the National Academy of Sciences, 113, 5797–5803, https://doi.org/10.1073/pnas.1514034112, 2016.

Després, V. R., Huffman, J. A., Burrows, S. M., Hoose, C., Safatov, A. S., Buryak, G., Fröhlich-Nowoisky, J., Elbert, W., Andreae, M. O., Pöschl, U., and Jaenicke, R.: Primary biological aerosol particles in the atmosphere: a review, Tellus B: Chemical and Physical Meteorology, https://doi.org/10.3402/tellusb.v64i0.15598, 2012.

Domine, F., Sparapani, R., Ianniello, A., and Beine, H. J.: The origin of sea salt in snow on Arctic sea ice and in coastal regions, Atmospheric Chemistry and Physics, 4, 2259–2271, https://doi.org/10.5194/acp-4-2259-2004, 2004.

Eirund, G. K., Possner, A., and Lohmann, U.: Response of Arctic mixed-phase clouds to aerosol perturbations under different surface forcings, Atmospheric Chemistry and Physics, 19, 9847–9864, https://doi.org/10.5194/acp-19-9847-2019, 2019.

Ewert, M., Carpenter, S. D., Colangelo-Lillis, J., and Deming, J. W.: Bacterial and extracellular polysaccharide content of brine-wetted snow over Arctic winter first-year sea ice, Journal of Geophysical Research: Oceans, 118, 726–735, https://doi.org/https://doi.org/10.1002/jgrc.20055, 2013.

Fan, S.-M. and Jacob, D. J.: Surface ozone depletion in Arctic spring sustained by bromine reactions on aerosols, Nature, 359, 522–524, https://doi.org/10.1038/359522a0, 1992.

Fetterer, F., Knowles, K., Meier, W. N., Savoie, M., Windnagel, A., and Stafford, T.: Sea Ice Index, Version 4, https://doi.org/10.7265/A98X-0F50, 2025.

Freitas, G. P., Adachi, K., Conen, F., Heslin-Rees, D., Krejci, R., Tobo, Y., Yttri, K. E., and Zieger, P.: Regionally sourced bioaerosols drive high-temperature ice nucleating particles in the Arctic, Nature Communications, 14, 5997, https://doi.org/10.1038/s41467-023-41696-7, 2023.

Frey, M. M., Norris, S. J., Brooks, I. M., Anderson, P. S., Nishimura, K., Yang, X., Jones, A. E., Nerentorp Mastromonaco, M. G., Jones, D. H., and Wolff, E. W.: First direct observation of sea salt aerosol production from blowing snow above sea ice, Atmospheric Chemistry and Physics, 20, 2549–2578, https://doi.org/10.5194/acp-20-2549-2020, 2020.

https://doi.org/10.5194/egusphere-2026-5047
Preprint. Discussion started: 26 August 2026

Garimella, S., Kristensen, T. B., Ignatius, K., Welti, A., Voigtländer, J., Kulkarni, G. R., Sagan, F., Kok, G. L., Dorsey, J., Nichman, L., Rothenberg, D. A., Rösch, M., Kirchgäßner, A. C. R., Ladkin, R., Wex, H., Wilson, T. W., Ladino, L. A., Abbatt, J. P. D., Stetzer, O., Lohmann, U., Stratmann, F., and Cziczo, D. J.: The SPectrometer for Ice Nuclei (SPIN): an instrument to investigate ice nucleation, Atmospheric Measurement Techniques, 9, 2781–2795, https://doi.org/10.5194/amt-9-2781-2016, 2016.

Gong, X., Zhang, J., and et al., B. C.: Arctic warming by abundant fine sea salt aerosols from blowing snow, Nature Geoscience, 16, 768—-774, 2023.

Hartmann, M., Blunier, T., Brügger, S., Schmale, J., Schwikowski, M., Vogel, A., Wex, H., and Stratmann, F.: Variation of Ice Nucleating Particles in the European Arctic Over the Last Centuries, Geophysical Research Letters, 46, 4007–4016, https://doi.org/https://doi.org/10.1029/2019GL082311, 2019.

Heutte, B., Bergner, N., Angot, H., Pernov, J. B., Dada, L., Mirrielees, J. A., Beck, I., Baccarini, A., Boyer, M., Creamean, J. M., Daellenbach, K. R., El Haddad, I., Frey, M. M., Henning, S., Laurila, T., Moschos, V., Petäjä, T., Pratt, K. A., Quéléver, L. L. J., Shupe, M. D., Zieger, P., Jokinen, T., and Schmale, J.: Observations of high-time-resolution and size-resolved aerosol chemical composition and microphysics in the central Arctic: implications for climate-relevant particle properties, Atmospheric Chemistry and Physics, 25, 2207–2241, https://doi.org/10.5194/acp-25-2207-2025, 2025.

Hill, M. K., Brooks, B. J., Norris, S. J., Smith, M. H., Brooks, I. M., and de Leeuw, G.: A Compact Lightweight Aerosol Spectrometer Probe (CLASP), Journal of Atmospheric and Oceanic Technology, 25, 1996 – 2006, https://doi.org/10.1175/2008JTECHA1051.1, 2008.

Hoose, C. and Möhler, O.: Heterogeneous ice nucleation on atmospheric aerosols: a review of results from laboratory experiments, Atmospheric Chemistry and Physics, 12, 9817–9854, 2012.

Huang, J. and Jaeglé, L.: Wintertime enhancements of sea salt aerosol in polar regions consistent with a sea ice source from blowing snow, Atmospheric Chemistry and Physics, 17, 3699–3712, 2017.

Jongebloed, U. A., Chalif, J. I., Tashmim, L., Porter, W. C., Bates, K. H., Chen, Q., Osterberg, E. C., Koffman, B. G., Cole-Dai, J., Winski, D. A., Ferris, D. G., Kreutz, K. J., Wake, C. P., and Alexander, B.: Dimethyl sulfide chemistry over the industrial era: comparison of key oxidation mechanisms and long-term observations, Atmospheric Chemistry and Physics, 25, 4083–4106, https://doi.org/10.5194/acp-25-4083-2025, 2025.

Kanji, Z. A., Ladino, L. A., Wex, H., Boose, Y., Burkert-Kohn, M., Cziczo, D. J., and Krämer, M.: Overview of Ice Nucleating Particles, Meteorological Monographs, 58, 1.1 – 1.33, https://doi.org/10.1175/AMSMONOGRAPHS-D-16-0006.1, 2017.

King, S. M., Butcher, A. C., Rosenoern, T., Coz, E., Lieke, K. I., de Leeuw, G., Nilsson, E. D., and Bilde, M.: Investigating Primary Marine Aerosol Properties: CCN Activity of Sea Salt and Mixed Inorganic–Organic Particles, Environmental Science & Technology, 46, 10 405–10 412, https://doi.org/10.1021/es300574u, 2012.

Korolev, A. and Field, P. R.: The Effect of Dynamics on Mixed-Phase Clouds: Theoretical Considerations, Journal of the Atmospheric Sciences, 65, 66 – 86, https://doi.org/10.1175/2007JAS2355.1, 2008.

Krumpen, T., von Albedyll, L., Goessling, H. F., Hendricks, S., Juhls, B., Spreen, G., Willmes, S., Belter, H. J., Dethloff, K., Haas, C., Kaleschke, L., Katlein, C., Tian-Kunze, X., Ricker, R., Rostosky, P., Rückert, J., Singha, S., and Sokolova, J.: MOSAiC drift expedition from October 2019 to July 2020: sea ice conditions from space and comparison with previous years, The Cryosphere, 15, 3897–3920, https://doi.org/10.5194/tc-15-3897-2021, 2021.

Lapere, R., Thomas, J. L., Marelle, L., Ekman, A. M. L., Frey, M. M., Lund, M. T., Makkonen, R., Ranjithkumar, A., Salter, M. E., Samset, B. H., Schulz, M., Sogacheva, L., Yang, X., and Zieger, P.: The Representation of Sea Salt Aerosols and Their Role in Polar Climate Within

https://doi.org/10.5194/egusphere-2026-5047
Preprint. Discussion started: 26 August 2026

CMIP6, Journal of Geophysical Research: Atmospheres, 128, e2022JD038 235, https://doi.org/https://doi.org/10.1029/2022JD038235, 2023.

Lawrence, Z. D., Perlwitz, J., Butler, A. H., Manney, G. L., Newman, P. A., Lee, S. H., and Nash, E. R.: The Remarkably Strong Arctic Stratospheric Polar Vortex of Winter 2020: Links to Record-Breaking Arctic Oscillation and Ozone Loss, Journal of Geophysical Research: Atmospheres, 125, e2020JD033 271, https://doi.org/https://doi.org/10.1029/2020JD033271, e2020JD033271 10.1029/2020JD033271, 2020.

Levine, J. G., Yang, X., Jones, A. E., and Wolff, E. W.: Sea salt as an ice core proxy for past sea ice extent: A process-based model study, Journal of Geophysical Research: Atmospheres, 119, 5737–5756, https://doi.org/https://doi.org/10.1002/2013JD020925, 2014.

Li, G., Welti, A., Thurnherr, I., Lohmann, U., and Kanji, Z. A.: Ice Nucleating Particle Concentrations over the Eurasian-Arctic seas, EGUsphere, 2025, 1–34, https://doi.org/10.5194/egusphere-2025-2798, 2025.

Li, L. and Pomeroy, J. W.: Estimates of Threshold Wind Speeds for Snow Transport Using Meteorological Data, Journal of Applied Meteorology, 36, 205 – 213, https://doi.org/10.1175/1520-0450(1997)036<0205:EOTWSF>2.0.CO;2, 1997.

Lubin, D. and Vogelmann, A.: A climatologically significant aerosol longwave indirect effect in the Arctic, Nature, 439, 453–456, https://doi.org/https://doi.org/10.1038/nature04449, 2006.

Macfarlane, A., Schneebeli, M., and et al, R. D.: A Database of Snow on Sea Ice in the Central Arctic Collected during the MOSAiC expedition, Sci Data, 10, https://doi.org/https://doi.org/10.1038/s41597-023-02273-1, 2023.

Marelle, L., Thomas, J. L., Ahmed, S., Tuite, K., Stutz, J., Dommergue, A., Simpson, W. R., Frey, M. M., and Baladima, F.: Implementation and Impacts of Surface and Blowing Snow Sources of Arctic Bromine Activation Within WRF-Chem 4.1.1, Journal of Advances in Modeling Earth Systems, 13, https://doi.org/https://doi.org/10.1029/2020MS002391, 2021.

Millero, F. J., Feistel, R., Wright, D. G., and McDougall, T. J.: The composition of Standard Seawater and the definition of the Reference-Composition Salinity Scale, Deep Sea Research Part I: Oceanographic Research Papers, 55, 50–72, https://doi.org/https://doi.org/10.1016/j.dsr.2007.10.001, 2008.

Möhler, O., Adams, M., Lacher, L., Vogel, F., Nadolny, J., Ullrich, R., Boffo, C., Pfeuffer, T., Hobl, A., Weiß, M., Vepuri, H. S. K., Hiranuma, N., and Murray, B. J.: The Portable Ice Nucleation Experiment (PINE): a new online instrument for laboratory studies and automated long-term field observations of ice-nucleating particles, Atmospheric Measurement Techniques, 14, 1143–1166, https://doi.org/10.5194/amt-14-1143-2021, 2021.

Morrison, H., Zuidema, P., Ackerman, A. S., Avramov, A., de Boer, G., Fan, J., Fridlind, A. M., Hashino, T., Harrington, J. Y., Luo, Y., Ovchinnikov, M., and Shipway, B.: Intercomparison of cloud model simulations of Arctic mixed-phase boundary layer clouds observed during SHEBA/FIRE-ACE, Journal of Advances in Modeling Earth Systems, 3, https://doi.org/https://doi.org/10.1029/2011MS000066, 2011.

Murphy, D. M. and Koop, T.: Review of the vapour pressures of ice and supercooled water for atmospheric applications, Quarterly Journal of the Royal Meteorological Society, 131, 1539–1565, https://doi.org/https://doi.org/10.1256/qj.04.94, 2005.

Nicolaus, M., Perovich, D. K., Spreen, G., Granskog, M. A., von Albedyll, L., Angelopoulos, M., Anhaus, P., Arndt, S., Belter, H. J., Bessonov, V., Birnbaum, G., Brauchle, J., Calmer, R., Cardellach, E., Cheng, B., Clemens-Sewall, D., Dadic, R., Damm, E., de Boer, G., Demir, O., Dethloff, K., Divine, D. V., Fong, A. A., Fons, S., Frey, M. M., Fuchs, N., Gabarró, C., Gerland, S., Goessling, H. F., Gradinger, R., Haapala, J., Haas, C., Hamilton, J., Hannula, H.-R., Hendricks, S., Herber, A., Heuzé, C., Hoppmann, M., Høyland, K. V., Huntemann, M., Hutchings, J. K., Hwang, B., Itkin, P., Jacobi, H.-W., Jaggi, M., Jutila, A., Kaleschke, L., Katlein, C., Kolabutin, N., Krampe, D., Kristensen, S. S., Krumpen, T., Kurtz, N., Lampert, A., Lange, B. A., Lei, R., Light, B., Linhardt, F., Liston, G. E., Loose, B., Macfarlane, A. R., Mahmud, M., Matero, I. O., Maus, S., Morgenstern, A., Naderpour, R., Nandan, V., Niubom, A., Oggier, M., Oppelt, N., Pätzold,

https://doi.org/10.5194/egusphere-2026-5047
Preprint. Discussion started: 26 August 2026

F., Perron, C., Petrovsky, T., Pirazzini, R., Polashenski, C., Rabe, B., Raphael, I. A., Regnery, J., Rex, M., Ricker, R., Riemann-Campe, K., Rinke, A., Rohde, J., Salganik, E., Scharien, R. K., Schiller, M., Schneebeli, M., Semmling, M., Shimanchuk, E., Shupe, M. D., Smith, M. M., Smolyanitsky, V., Sokolov, V., Stanton, T., Stroeve, J., Thielke, L., Timofeeva, A., Tonboe, R. T., Tavri, A., Tsamados, M., Wagner, D. N., Watkins, D., Webster, M., and Wendisch, M.: Overview of the MOSAiC expedition: Snow and sea ice, Elementa: Science of the Anthropocene, 10, 000 046, https://doi.org/10.1525/elementa.2021.000046, 2022.

Nilsson, E. D., Rannik, , Swietlicki, E., Leck, C., Aalto, P. P., Zhou, J., and Norman, M.: Turbulent aerosol fluxes over the Arctic Ocean: 2. Wind-driven sources from the sea, Journal of Geophysical Research: Atmospheres, 106, 32 139–32 154, https://doi.org/https://doi.org/10.1029/2000JD900747, 2001.

Nishimura, K., Yokoyama, C., Ito, Y., Nemoto, M., Naaim-Bouvet, F., Bellot, H., and Fujita, K.: Snow particle speeds in drifting snow, Journal of Geophysical Research: Atmospheres, 119, 9901–9913, https://doi.org/https://doi.org/10.1002/2014JD021686, 2014.

Nixdorf, U., Dethloff, K., Rex, M., Shupe, M., Sommerfeld, A., Perovich, D. K., Nicolaus, M., Heuzé, C., Rabe, B., Loose, B., Damm, E., Gradinger, R., Fong, A., Maslowski, W., Rinke, A., Kwok, R., Spreen, G., Wendisch, M., Herber, A., Hirsekorn, M., Mohaupt, V., Frickenhaus, S., Immerz, A., Weiss-Tuider, K., König, B., Mengedoht, D., Regnery, J., Gerchow, P., Ransby, D., Krumpen, T., Morgenstern, A., Haas, C., Kanzow, T., Rack, F. R., Saitzev, V., Sokolov, V., Makarov, A., Schwarze, S., Wunderlich, T., Wurr, K., and Boetius, A.: MOSAiC Extended Acknowledgement, https://doi.org/10.5281/zenodo.5541624, 2021.

Norris, S. J., Brooks, I. M., de Leeuw, G., Smith, M. H., Moerman, M., and Lingard, J. J. N.: Eddy covariance measurements of sea spray particles over the Atlantic Ocean, Atmospheric Chemistry and Physics, 8, 555–563, https://doi.org/10.5194/acp-8-555-2008, 2008.

Overland, J., Dunlea, E., Box, J. E., Corell, R., Forsius, M., Kattsov, V., Olsen, M. S., Pawlak, J., Reiersen, L.-O., and Wang, M.: The urgency of Arctic change, Polar Science, 21, 6–13, https://doi.org/https://doi.org/10.1016/j.polar.2018.11.008, iSAR-5/ Fifth International Symposium on Arctic Research, 2019.

Peng, S., Yang, Q., Shupe, M. D., Xi, X., Han, B., Chen, D., Dahlke, S., and Liu, C.: The characteristics of atmospheric boundary layer height over the Arctic Ocean during MOSAiC, Atmospheric Chemistry and Physics, 23, 8683–8703, https://doi.org/10.5194/acp-23-8683-2023, 2023.

Perovich, D., Meier, W., Tschudi, M., Hendricks, S., Petty, A. A., Divine, D., Farrell, S., Gerland, S., Haas, C., Kaleschke, L., Pavlova, O., Ricker, R., Tian-Kunze, X., Webster, M., and Wood, K.: Arctic Report Card 2020: Sea Ice, Tech. rep., National Oceanic and Atmospheric Administration, Office of Oceanic and Atmospheric Research, Pacific Marine Environmental Laboratory, https://doi.org/10.25923/n170-9h57, 2020.

Polen, M., Brubaker, T., Somers, J., and Sullivan, R. C.: Cleaning up our water: reducing interferences from nonhomogeneous freezing of "pure" water in droplet freezing assays of ice-nucleating particles, Atmospheric Measurement Techniques, 11, 5315–5334, https://doi.org/10.5194/amt-11-5315-2018, 2018.

Pöschl, U., Martin, S. T., Sinha, B., Chen, Q., Gunthe, S. S., Huffman, J. A., Borrmann, S., Farmer, D. K., Garland, R. M., Helas, G., Jimenez, J. L., King, S. M., Manzi, A., Mikhailov, E., Pauliquevis, T., Petters, M. D., Prenni, A. J., Roldin, P., Rose, D., Schneider, J., Su, H., Zorn, S. R., Artaxo, P., and Andreae, M. O.: Rainforest Aerosols as Biogenic Nuclei of Clouds and Precipitation in the Amazon, Science, 329, 1513–1516, https://doi.org/10.1126/science.1191056, 2010.

Ranjithkumar, A.: Snow particle number, aerosol concentration and 10 meter windspeed data from MOSAiC, N-ICE, Weddel Sea expeditions and chemistry transport model data (p-TOMCAT), https://doi.org/10.5281/zenodo.13760111, 2024.

https://doi.org/10.5194/egusphere-2026-5047
Preprint. Discussion started: 26 August 2026

Ranjithkumar, A., Duncan, E., Yang, X., Partidge, D., Lachlan-Cope, T., Gong, X., Nishimura, K., and Frey, M.: Direct observation of Arctic Sea salt aerosol production from blowing snow and modeling over a changing sea ice environment, Elementa: Science of the Anthropocene, 13, https://doi.org/10.1525/elementa.2024.00006, 2025.

Rantanen, M., Karpechko, A., Lipponen, A., Nordling, K., Hyvärinen, O., Ruosteenoja, K., Vihma, T., and Laaksonen, A.: The Arctic has warmed nearly four times faster than the globe since 1979, Communications Earth Environment, 3, https://doi.org/10.1038/s43247-022-00498-3, 2022.

Rhodes, R., Yang, X., Wolff, E., McConnell, J., and Frey, M.: Sea ice as a source of sea salt aerosol to Greenland ice cores: a model-based study, Atmospheric Chemistry and Physics, 17, 9417–9433, 2017.

Richter, A., Wittrock, F., Eisinger, M., and Burrows, J. P.: GOME observations of tropospheric BrO in northern hemispheric spring and summer 1997, Geophysical Research Letters, 25, 2683–2686, https://doi.org/https://doi.org/10.1029/98GL52016, 1998.

Robinson, J., Jaeglé, L., Palm, S. P., Shupe, M. D., Liston, G. E., and Frey, M. M.: ICESat-2 Observations of Blowing Snow Over Arctic Sea Ice During the 2019–2020 MOSAiC Expedition, Journal of Geophysical Research: Atmospheres, 130, e2025JD043 919, https://doi.org/https://doi.org/10.1029/2025JD043919, 2025.

Schmale, J., Zieger, P., and Ekman, A.: Aerosols in current and future Arctic climate, Nature Climate Change, 11, 95–105, 2021.

Serreze, M. and Barry, R.: Processes and impacts of Arctic amplification: A research synthesis, Global and Planetary Change, 77, 85–96, 2011.

Shaw, G. E.: The Arctic Haze Phenomenon, Bulletin of the American Meteorological Society, 76, 2403 – 2414, https://doi.org/10.1175/1520-0477(1995)076<2403:TAHP>2.0.CO;2, 1995.

Shupe, M. D., Rex, M., Blomquist, B., Persson, P. O. G., Schmale, J., Uttal, T., Althausen, D., Angot, H., Archer, S., Bariteau, L., Beck, I., Bilberry, J., Bucci, S., Buck, C., Boyer, M., Brasseur, Z., Brooks, I. M., Calmer, R., Cassano, J., Castro, V., Chu, D., Costa, D., Cox, C. J., Creamean, J., Crewell, S., Dahlke, S., Damm, E., de Boer, G., Deckelmann, H., Dethloff, K., Dütsch, M., Ebell, K., Ehrlich, A., Ellis, J., Engelmann, R., Fong, A. A., Frey, M. M., Gallagher, M. R., Ganzeveld, L., Gradinger, R., Graeser, J., Greenamyer, V., Griesche, H., Griffiths, S., Hamilton, J., Heinemann, G., Helmig, D., Herber, A., Heuzé, C., Hofer, J., Houchens, T., Howard, D., Inoue, J., Jacobi, H.-W., Jaiser, R., Jokinen, T., Jourdan, O., Jozef, G., King, W., Kirchgaessner, A., Klingebiel, M., Krassovski, M., Krumpen, T., Lampert, A., Landing, W., Laurila, T., Lawrence, D., Lonardi, M., Loose, B., Lüpkes, C., Maahn, M., Macke, A., Maslowski, W., Marsay, C., Maturilli, M., Mech, M., Morris, S., Moser, M., Nicolaus, M., Ortega, P., Osborn, J., Pätzold, F., Perovich, D. K., Petäjä, T., Pilz, C., Pirazzini, R., Posman, K., Powers, H., Pratt, K. A., Preußer, A., Quéléver, L., Radenz, M., Rabe, B., Rinke, A., Sachs, T., Schulz, A., Siebert, H., Silva, T., Solomon, A., Sommerfeld, A., Spreen, G., Stephens, M., Stohl, A., Svensson, G., Uin, J., Viegas, J., Voigt, C., von der Gathen, P., Wehner, B., Welker, J. M., Wendisch, M., Werner, M., Xie, Z., and Yue, F.: Overview of the MOSAiC expedition: Atmosphere, Elementa: Science of the Anthropocene, 10, 00 060, https://doi.org/10.1525/elementa.2021.00060, 2022.

Sirois, A. and Barrie, L. A.: Arctic lower tropospheric aerosol trends and composition at Alert, Canada: 1980–1995, Journal of Geophysical Research: Atmospheres, 104, 11 599–11 618, https://doi.org/https://doi.org/10.1029/1999JD900077, 1999.

Ström, J., Umegård, J., Tørseth, K., Tunved, P., Hansson, H.-C., Holmén, K., Wismann, V., Herber, A., and König-Langlo, G.: One year of particle size distribution and aerosol chemical composition measurements at the Zeppelin Station, Svalbard, March 2000–March 2001, Physics and Chemistry of the Earth, Parts A/B/C, 28, 1181–1190, https://doi.org/https://doi.org/10.1016/j.pce.2003.08.058, the changing physical environment of Ny-Alesund Svalbard, 2003.

https://doi.org/10.5194/egusphere-2026-5047
Preprint. Discussion started: 26 August 2026

Sze, K. C. H., Wex, H., Hartmann, M., Skov, H., Massling, A., Villanueva, D., and Stratmann, F.: Ice-nucleating particles in northern Greenland: annual cycles, biological contribution and parameterizations, Atmospheric Chemistry and Physics, 23, 4741–4761, https://doi.org/10.5194/acp-23-4741-2023, 2023.

Tobo, Y., Adachi, K., Kawai, K., Matsui, H., Ohata, S., Oshima, N., Kondo, Y., Hermansen, O., Uchida, M., Inoue, J., and Koike, M.: Surface warming in Svalbard may have led to increases in highly active ice-nucleating particles, Communications Earth Environment, 5, https://doi.org/10.1038/s43247-024-01677-0, 2024.

Twomey, S.: The Influence of Pollution on the Shortwave Albedo of Clouds, Journal of Atmospheric Sciences, 34, 1149 – 1152, https://doi.org/10.1175/1520-0469(1977)034<1149:TIOPOT>2.0.CO;2, 1977.

Vali, G.: Quantitative Evaluation of Experimental Results an the Heterogeneous Freezing Nucleation of Supercooled Liquids, Journal of Atmospheric Sciences, 28, 402 – 409, https://doi.org/10.1175/1520-0469(1971)028<0402:QEOERA>2.0.CO;2, 1971.

Wagenbach, D., Ducroz, F., Mulvaney, R., Keck, L., Minikin, A., Legrand, M., Hall, J. S., and Wolff, E. W.: Sea-salt aerosol in coastal Antarctic regions, Journal of Geophysical Research: Atmospheres, 103, 10 961–10 974, https://doi.org/https://doi.org/10.1029/97JD01804, 1998.

Wex, H., Huang, L., Zhang, W., Hung, H., Traversi, R., Becagli, S., Sheesley, R. J., Moffett, C. E., Barrett, T. E., Bossi, R., Skov, H., Hünerbein, A., Lubitz, J., Löffler, M., Linke, O., Hartmann, M., Herenz, P., and Stratmann, F.: Annual variability of ice-nucleating particle concentrations at different Arctic locations, Atmospheric Chemistry and Physics, 19, 5293–5311, https://doi.org/10.5194/acp-19-5293-2019, 2019.

Wolff, E. W., Rankin, A. M., and Röthlisberger, R.: An ice core indicator of Antarctic sea ice production?, Geophysical Research Letters, 30, https://doi.org/https://doi.org/10.1029/2003GL018454, 2003.

Yang, X., Pyle, J. A., and Cox, R. A.: Sea salt aerosol production and bromine release: Role of snow on sea ice, Geophysical Research Letters, 35, https://doi.org/https://doi.org/10.1029/2008GL034536, 2008.

Yang, X., Frey, M. M., Rhodes, R. H., Norris, S. J., Brooks, I. M., Anderson, P. S., Nishimura, K., Jones, A. E., and Wolff, E. W.: Sea salt aerosol production via sublimating wind-blown saline snow particles over sea ice: parameterizations and relevant microphysical mechanisms, Atmospheric Chemistry and Physics, 19, 8407–8424, https://doi.org/10.5194/acp-19-8407-2019, 2019.

Yang, X., Strong, K., Criscitiello, A. S., Santos-Garcia, M., Bognar, K., Zhao, X., Fogal, P., Walker, K. A., Morris, S. M., and Effertz, P.: Surface snow bromide and nitrate at Eureka, Canada, in early spring and implications for polar boundary layer chemistry, Atmospheric Chemistry and Physics, 24, 5863–5886, https://doi.org/10.5194/acp-24-5863-2024, 2024.

Zeppenfeld, S., Schmidt, L., and van Pinxteren, M.: Major Inorganic and Selected Organic Ions in Total Suspended Aerosol Particles During the MOSAiC Drift (2019/2020) in the High Arctic, https://doi.org/10.1594/PANGAEA.973882, 2024.